
Interpretable Causal Graphical Models for Equilibrium Systems with Confounding

Kai Z. Teh,* Kayvan Sadeghi and Terry Soo

Department of Statistical Science, University College London, Gower Street, WC1E 6BT, London, UK

*Email for correspondence. kai.teh.21@ucl.ac.uk

Abstract

In applications, quantities of interest are often modelled in equilibrium or an equilibrium solution is sought. The presence of confounding makes causal inference in this setting challenging. We provide interpretable graphical models for equilibrium systems with confounding using arterial graphs (Lauritzen and Sadeghi, 2018), a class of graphs containing directed acyclic graphs, ancestral graphs, and chain graphs. In this setting, we provide valid graphical representations of both counterfactual variables and observational variables, which we relate to counterfactual graphs (Shpitser and Pearl, 2007) and single-world intervention graphs (Richardson and Robins, 2013). As an application of this graphical representation, we provide an element-wise procedure of selecting adjustment sets that flexibly include and exclude given covariates.

Key words: Causal Inference, Graphical Models, Gibbs Sampler, Confounding

1. Introduction

Causal inference aims to predict the consequences of interventions in the form of causal effects. When interventional data from randomised control trials are unavailable, causal assumptions relating observational data to the intervened setting are required to estimate causal effects.

A prominent casual inference framework that captures these assumptions is the graphical model formulation by Pearl (2009), based on directed acyclic graphs (DAGs) interpreted as structural causal models (SCMs). Edges in a DAG are all directed and thus are not suitable in capturing symmetric relations between variables such as relationships induced by equilibria and confounding. Ancestral graphs (Richardson and Spirtes, 2002) and chain graphs (Frydenberg, 1990) have been proposed to represent confounding (Richardson and Spirtes, 2002; Zhang, 2008) (see also Sadeghi and Soo (2022)) or variables at equilibrium (Lauritzen and Richardson, 2002).

Arterial graphs (Lauritzen and Sadeghi, 2018) provide a natural generalisation of chain graphs, ancestral graphs, and DAGs, and also represent the marginalisation and conditioning of these classes of graphs (Sadeghi, 2016). In addition to directed edges, arterial graphs also contain bidirected and undirected edges, which we will use to represent confounding and equilibrium relationships between variables, respectively. We will formalise these confounding and equilibrium relationships using a generalisation of SCMs.

Our arterial graphical model thus enables causal inference for equilibrium systems with confounding, and unifies and generalises causal graphical models described by Richardson and Spirtes (2002); Zhang (2008) and Lauritzen and Richardson (2002), for ancestral graphs and chain graphs, respectively. Causal inference using arterial graphs is also interpretable since causal notions such as interventions can be expressed purely graphically as local mechanistic manipulations on the intervened variables. To demonstrate this interpretability, in the same spirit as counterfactual graphs (Shpitser and Pearl, 2007) and single-world intervention graphs (Richardson and Robins, 2013), we will provide graphs that encode counterfactual conditional independence assumptions between observational variables and counterfactual variables in the case of arterial graphs.

These counterfactual conditional independencies encode many important assumptions for methods in causal inference. One such assumption is the conditional exchangeability assumption (Hernan and Robins,

2020), which is important in tasks such as selecting an adjustment set of confounder covariates to control for confounding between treatment and outcome variables. A variety of criteria have been proposed to select such a set of confounder covariates, such as the backdoor criterion of Pearl (2009, Chapter 3.3.1) and the pre-treatment heuristics of Rubin (2009). Recently, there has also been work addressing other aspects of such selection criteria, such as statistical efficiency (Rotnitzky and Smucler, 2020) and the limited structural knowledge of the underlying causal graph (Guo and Zhao, 2026).

Based on marginalisation and conditioning operations developed for ancestral graphs (Sadeghi, 2016), we provide an element-wise algorithm to select an adjustment set constrained to include and exclude given covariates, which can arise in practice due to prohibitive costs or regulation requirements in areas such as clinical trials or algorithmic fairness. Our algorithm is provably correct under conditions such as when the counterfactual graphs provided is valid. Compared to standard approaches of selecting adjustment sets where the inclusion and exclusion constraints are enforced post-hoc, after efficiently enumerating all possible adjustment sets (van der Zander et al., 2019), our approach takes the constraints into account directly in the algorithm.

The structure of the paper will be as follows: Section 2 covers the relevant background, Section 3 covers the ancestral graphical model of equilibrium systems with confounding, Section 4 covers interventions and the extension of counterfactual graphs in this setting using our ancestral graphical model, and Section 5 covers the confounder selection algorithm. All proofs will be deferred to the final section.

2. Background

2.1. Probabilistic Graphs

Let \mathcal{G} denote a graph over a finite set of nodes V , with only one of the three types of edges: *directed* (\rightarrow), *undirected* ($-$), and *bidirected* (\leftrightarrow), connecting two adjacent nodes. Consider a sequence $\langle i_0, \dots, i_n \rangle$ of nodes in the graph \mathcal{G} . If every pair of consecutive nodes is adjacent, then the sequence is a *path*; if $i_0 = i_n$, in addition, then the sequence is a *cycle*. If each edge between consecutive adjacent nodes i_m and i_{m+1} is either undirected or directed as $i_m \rightarrow i_{m+1}$, then the sequence is a *semi-directed path* from i_0 to i_n ; if in addition $i_0 = i_n$ and at least one of the edges is directed, then the sequence is a *semi-directed cycle*.

In this work, we will consider *ancestral graphs* (Lauritzen and Sadeghi, 2018).

Definition 1 (Ancestral graphs) An ancestral graph over a set of nodes is a graph which may contain directed, undirected, and bidirected edges that satisfies the following.

1. There does not exist a semi-directed path between two nodes that are adjacent via a bidirected edge.
2. The graph does not contain semi-directed cycles.

By allowing only directed edges, we recover the definition of a *directed acyclic graph* (DAG). Likewise excluding bidirected edges or node configurations of the form $i - k \leftrightarrow j$ (which is trivially satisfied by excluding undirected edges), we recover the definition of chain graphs or ancestral graphs, respectively.

Following Frydenberg (1990), a *chain component* τ in an ancestral graph \mathcal{G} is a maximal set of nodes such that every pair of nodes $x, y \in \tau$ is connected by a sequence of undirected edges; thus all nodes in \mathcal{G} can be partitioned into chain components. Note that in the case of a DAG, each node is a chain component. Given a node $i \in V$, let $\tau(i)$ denote the chain component containing i . Given a set of nodes $C \subseteq V$ in a graph \mathcal{G} , the *neighbors* of C , denoted by $\text{ne}(C)$, are the set of nodes $x \notin C$ such that $x - i$ for some node $i \in C$; the *parents* of C , denoted by $\text{pa}(C)$, are the set of nodes $x \notin C$ such that $x \rightarrow i$ for some node $i \in C$; the *anterior* of C , denoted by $\text{ant}(C)$, is the set of nodes $x \notin C$ such that there exists a semi-directed path from x to some node $i \in C$.

Remark 1 *When undirected edges are absent, the anterior of C coincides with the ancestors of C . Note that some authors let the neighbors and anterior of the set $C \subseteq V$ contain the set C itself, however, we do not.* \diamond

For disjoint subsets $A, B, C \subseteq V$, let $A \perp_{\mathcal{G}} B \mid C$ denote the graphical separation of A and B given C in a graph \mathcal{G} ; in the case of ancestral graphs, this is understood as the separation criterion in Lauritzen and Sadeghi (2018, Section 3.2), which is simplified to the classical d-separation (Pearl, 2009, Chapter 1.2.3)

when the graph \mathcal{G} is a DAG, and m-separation for ancestral graphs; see also Lauritzen and Sadeghi (2018, Section 3.3). For brevity, we will sometimes express the singleton set $\{i\} \subseteq V$, without the set braces, as i . The graphs \mathcal{G}_1 and \mathcal{G}_2 over the same node set V are *Markov equivalent* if they induce the same graphical separations.

In a DAG, each pair of non-adjacent nodes are separated, say by their ancestors. However, an anterial graph need not be *maximal* (see the graph \mathcal{G}_0^* in Figure 11 for example).

Definition 2 (Maximal graphs) A graph \mathcal{G} is maximal if for each pair of nodes i and j in \mathcal{G} , we have

$$i \text{ not adjacent to } j \text{ in } \mathcal{G} \Rightarrow i \perp_{\mathcal{G}} j \mid C \text{ for some } C \subseteq V \setminus \{i, j\}.$$

Lauritzen and Sadeghi (2018) characterised when anterial graphs are maximal. They also provided a graphical operation $\max(\cdot)$ which *maximises* any given anterial graph \mathcal{G} —returning a graph $\max(\mathcal{G})$ with the following properties.

- The graph $\max(\mathcal{G})$ is maximal.
- The graphs $\max(\mathcal{G})$ and \mathcal{G} are Markov equivalent.
- The graph \mathcal{G} is a subgraph of $\max(\mathcal{G})$.

We associate a set of random variables $X_V = (X_1, \dots, X_{|V|})$ with a joint distribution P to the set of nodes V . We will often write $X \sim P$, if P is the law of X . Given a set $A \subseteq V$, let $X_A = (X_i)_{i \in A}$, and $A \perp\!\!\!\perp B \mid C$ denote the conditional independence of X_A and X_B given X_C . If each graphical separation implies a corresponding conditional independence, then we have the *Markov property*:

Definition 3 (Markov property) A distribution P is Markovian to \mathcal{G} if $A \perp_{\mathcal{G}} B \mid C \Rightarrow A \perp\!\!\!\perp B \mid C$ for all disjoint $A, B, C \subseteq V$.

If we have the reverse implication as well, then we have *faithfulness*.

Definition 4 (Faithfulness) A distribution P is faithful to \mathcal{G} if $A \perp_{\mathcal{G}} B \mid C \iff A \perp\!\!\!\perp B \mid C$ for all disjoint $A, B, C \subseteq V$.

If the distribution P is faithful to some anterial graph \mathcal{G} , then P is a compositional graphoid (Sadeghi, 2017, Theorem 17).

Definition 5 (Compositional graphoid) A distribution P over V is a compositional graphoid if we have the following conditional independence properties. For disjoint $A, B, C, D \subseteq V$,

- (Intersection) $A \perp\!\!\!\perp B \mid C \cup D$ and $A \perp\!\!\!\perp D \mid C \cup B$ implies $A \perp\!\!\!\perp B \cup D \mid C$, and
- (Composition) $A \perp\!\!\!\perp B \mid C$ and $A \perp\!\!\!\perp D \mid C$ implies $A \perp\!\!\!\perp B \cup D \mid C$.

Remark 2 Examples of compositional graphoids are given by multivariate Gaussian distributions. The assumption that a distribution is a compositional graphoid is often made when attempting to faithfully describe a distribution via a graphical model; see Sadeghi (2017). \diamond

Given a distribution P over variables X_V , disjoint subsets $M, C \subseteq V$ and x_B , a fixed value of X_B , let $P_A(\cdot \mid x_B)$ denote the marginal of the conditional distribution $P(\cdot \mid x_B)$ over X_A (by integrating out $X_{V \setminus (A \cup B)}$). For a distribution P_V that is faithful to a DAG \mathcal{G} , there does not necessarily exist a DAG to which the marginal distribution $P_{V \setminus M}$ is faithful. Likewise, there does not necessarily exist a DAG to which the conditional distribution $P(\cdot \mid x_C)$ is faithful.

In the case where P is faithful to an anterial graph \mathcal{G} , anterial graphs to which the marginal or conditional distributions are faithful always exist. Anterial graphs are thus closed under marginalising and conditioning, unlike DAGs, chain graphs and ancestral graphs. Given an anterial graph \mathcal{G} over the nodes V and subset $M \subseteq V$, Sadeghi (2016) provides the graphical operation α_m to marginalise \mathcal{G} , which

returns the antieral graph $\alpha_m(\mathcal{G}; M)$ over nodes $V \setminus M$ such that for disjoint $A, B, C \subseteq V \setminus M$, we have

$$A \perp_{\mathcal{G}} B | C \iff A \perp_{\alpha_m(\mathcal{G}; M)} B | C. \quad (1)$$

This correspondence captures the relationship between the conditional independencies of a distribution P and its marginal distribution $P_{V \setminus M}$.

Similarly with conditioning, given any antieral graph \mathcal{G} over the nodes V and a subset $C \subseteq V$, Sadeghi (2016) provides the graphical operation α_c to condition \mathcal{G} , which returns the antieral graph $\alpha_c(\mathcal{G}; C)$ over nodes $V \setminus C$ such that for disjoint $A, B, D \subseteq V \setminus C$, we have

$$A \perp_{\mathcal{G}} B | D \cup C \iff A \perp_{\alpha_c(\mathcal{G}; C)} B | D. \quad (2)$$

This correspondence captures the relationship between the conditional independencies of a distribution P and its conditional distribution $P(\cdot | x_C)$.

We will be using these properties of marginalisation and conditioning to analyse the confounder selection algorithm proposed in Section 5; see Theorem 5 for Algorithm 4.

2.2. Interventions and Confounder Selection

A DAG \mathcal{G} is often associated to a *structural causal model* with mutually independent errors.

Definition 6 (Structural causal model (SCM)) Let \mathcal{G} be a DAG where every node i is associated with a function f_i and an error random variable ϵ_i . An SCM consists of functional assignments recursively defining observational random variables X_V of the form $X_i = f_i(X_{\text{pa}(i)}, \epsilon_i)$, for every node $i \in V$.

We let P be the law of X_V , so that P is the observational distribution. When the errors are mutually independent, the resulting joint distribution P is Markovian to the DAG \mathcal{G} (Pearl, 2009, Theorem 1.4.1); this result facilitates the use of graphical calculus on DAGs to manipulate the SCM for the purposes of causal inference, such as in the case of adjustment set selection. We will prove an analogue of this result when the distribution P is induced via SCMs of equilibriums with confounding; see Theorem 1.

Using an SCM, intervening on a treatment set $C \subseteq V$ amounts to replacing the functional assignments of all X_i where $i \in C$ with some fixed values a_i , while keeping the functional assignments of all X_j where $j \notin C$ fixed. This replacement results in the definition of a different set of intervened random variables $X_V^{\text{do}(a_C)} = (X_1^{\text{do}(a_C)}, \dots, X_{|V|}^{\text{do}(a_C)})$, with which we associate an interventional distribution $P^{\text{do}(a_C)}$. The new variables $X_V^{\text{do}(a_C)}$ will be referred to as intervened variables in the scope of this work. Note that $X_V^{\text{do}(a_C)}$ are also known as potential outcomes (Rubin, 1978, 2005).

Let $O \subseteq V$ denote the outcome set and X_C the treatment variables. Expressing common causal estimands such as the *conditional average treatment effect* (CATE) solely in terms of the observational distribution depend on the following *unconfoundedness* assumption: there exists an *adjustment set* $S \subseteq V$ such that

$$X_O^{\text{do}(a_C)} \perp\!\!\!\perp X_C | X_S \quad (3)$$

holds for all possible intervened values a_C . If there is no subset of S that satisfies (3), then S is *minimal*. The conditional independence (3) is also known as the conditional exchangability condition (Hernan and Robins, 2020, Page 18).

Graphically, this coupling has been described using approaches such as twin-networks (Balke and Pearl, 1994), counterfactual graphs, (Shpitser and Pearl, 2007) and single-world intervention graphs (Richardson and Robins, 2013, 2023). These methods represent observational and intervened variables in a single graph \mathcal{G}' so that conditional independence relations between observational and intervened variables, such as (3), can be expressed as classical d-separation in \mathcal{G}' .

Note that (3) requires that the *joint* distribution of the intervened outcome variable $X_O^{\text{do}(a_C)}$ and the observational variable X_C to be well-defined; the required coupling between observational and intervened variables is specified by the shared errors ϵ_V between the SCM and the intervened SCM.

In this work, we will only be concerned with the kind of counterfactual assumptions that relate observational variables X_V and intervened variables $X_V^{\text{do}(a_C)}$ where the intervened value a_C is fixed, such as (3); relating intervened variables $X_V^{\text{do}(a_C)}$ and $X_V^{\text{do}(a'_C)}$ for different values a_C and a'_C is outside of our scope. Thus, we will consider only the set of treatment variables C and not the actual values a_C of the intervention, and this will be suppressed in our notation as $X_V^{\text{do}(C)}$ and $P^{\text{do}(C)}$. Note that such assumptions are still sufficient for expressing some of the causal estimands involving different intervened values such as the *effect of treatment on the treated* (ETT).

2.3. Causal Interpretation of Chain Graphs

Given a chain graph \mathcal{G} , based on the factorisation property of chain graphs (Frydenberg, 1990), Lauritzen and Richardson (2002) has proposed causal interpretations of chain graphs as a data generating process having two nested processes. The outer process expresses the relationship between different chain components as

$$X_\tau = f_\tau(X_{\text{pa}(\tau)}, \epsilon_\tau) \quad (4)$$

for some random error variable ϵ_τ associated to each chain component τ , where the errors are jointly independent. These can be understood as SCM functional assignments by considering the chain component as nodes in a DAG. The inner process then associates each chain component τ with a dynamical process that has a conditional equilibrium distribution given $x_{\text{pa}(\tau)}$.

3. Structured Equilibrium Models with Confounding

We will formally express the relationship between different chain components described in (4) with potential confounding, as a structural equilibrium model.

Definition 7 (Structural equilibrium model) Let τ_1, \dots, τ_n be the parts of an ordered partition of V . Each part τ_i is associated with a function f_{τ_i} with arguments $X_{\text{pa}(\tau_i)}$, where $\text{pa}(\tau_i) \subseteq \{\tau_1, \dots, \tau_{i-1}\}$, and an error random variable ϵ_{τ_i} . A structural equilibrium model consists of functional assignments of observational random variables X_{τ_i} of the following form

$$X_{\tau_i} = f_{\tau_i}(X_{\text{pa}(\tau_i)}, \epsilon_{\tau_i}).$$

Note that the errors $\epsilon_{\tau_1}, \dots, \epsilon_{\tau_n}$ need not be jointly independent. If all τ_1, \dots, τ_n are all singletons with jointly independent errors, then we recover the definition of an SCM for DAGs—in this case, Lauritzen and Richardson (2002, Section 6.3) view Definition 7 as a data generating process

The notation $\text{pa}(\tau_i)$ suggests a corresponding graph \mathcal{G} . Indeed, given a structural equilibrium model, we construct the corresponding graph \mathcal{G} by considering, for each part $\tau \in \{\tau_1, \dots, \tau_n\}$, how τ is connected to $\text{pa}(\tau)$ based on the functional assignment of τ . This construction is formalised as Algorithm 1.

Algorithm 1 The corresponding graph \mathcal{G} of a structural equilibrium model

Input: Structural equilibrium model

Output: Graph \mathcal{G} .

- For every part $\tau \in \{\tau_1, \dots, \tau_n\}$, let $J^\tau(\cdot | x_{\text{pa}(\tau)})$ be the law of $f_\tau(x_{\text{pa}(\tau)}, \epsilon_\tau)$.
 - 1: For nodes i and j in τ , if $i \not\perp\!\!\!\perp j | \tau \setminus \{i, j\}$ holds for $J^\tau(\cdot | x_{\text{pa}(\tau)})$, then add undirected edge $i - j$.
 - 2: For nodes $i \in \text{pa}(\tau)$ and $j \in \tau$, if for all values of $x_{(\tau \cup \text{pa}(\tau)) \setminus \{i, j\}}$, the conditional marginal $J_i^\tau(\cdot | x_{\tau \setminus i}; x_{\text{pa}(\tau)})$ depends on the value of x_i , then add the directed edge $i \rightarrow j$.
 - 3: For parts τ and τ' , if $\epsilon_\tau \not\perp\!\!\!\perp \epsilon_{\tau'}$, then add bidirected edges $i \leftrightarrow j$ for every node $i \in \tau$ and $j \in \tau'$.
-

For examples of structural equilibrium models and their corresponding graphs, see Figures 4, 5, and 6 in Section 3.2.

Remark 3 *Step 1 of Algorithm 1 ensures that $J^\tau(\cdot | x_{\text{pa}(\tau)})$ satisfies the pairwise Markov property with respect to (w.r.t.) to the constructed undirected graph over nodes in τ and that no subgraph of the undirected graph satisfies this property.*

The condition in Step 2 of Algorithm 1 can be succinctly expressed as $i \not\perp\!\!\!\perp j | \tau \cup \text{pa}(\tau) \setminus \{i, j\}$ using the formulation in Constantinou and Dawid (2017, Theorem 3.5), which allows the expression of dependence on fixed parameters $x_{\text{pa}(\tau)}$ as an extended conditional independence statement. These (extended) conditional independencies over τ and $\text{pa}(\tau)$ are represented graphically using Algorithm 1. See Figure 1. \diamond

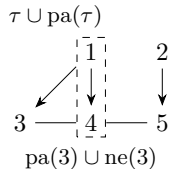


Fig. 1: Chain component $\tau = \{3, 4, 5\}$ and parents $\text{pa}(\tau) = \{1, 2\}$. For every node $i \in \tau$, Algorithm 1 constructs $\text{ne}(i)$ and $\text{pa}(i)$ such that the conditional marginal $J_i^\tau(\cdot | x_{\tau \setminus i}; x_{\text{pa}(\tau)})$ does not depend on nodes outside of $\text{pa}(i) \cup \text{ne}(i)$ (formalised as Lemma 10 in the Proofs Section).

For every part τ , Step 1 of Algorithm 1 constructs the chain components of the graph \mathcal{G} using the distribution $J^\tau(\cdot | x_{\text{pa}(\tau)})$ of $f_\tau(x_{\text{pa}(\tau)}, \epsilon_\tau)$ from the model. For every node $i \in \tau$, step 2 of Algorithm 1 then uses the i -marginal of the conditional distribution $J_i^\tau(\cdot | x_{\text{ne}(i)}; x_{\text{pa}(\tau)})$ to determine the parents of i for the constructed \mathcal{G} . Step 3 of the algorithm then includes bidirected edges in the constructed graph \mathcal{G} to represent dependent noises of the model.

Remark 4 (Relating parts to chain components of \mathcal{G}) *Consider the part τ that decomposes in multiple connected components τ'_1, \dots, τ'_m after performing Step 1 of Algorithm 1. These connected components are the chain components of the corresponding graph \mathcal{G} .*

Since Step 1 of Algorithm 1 constructs an undirected graph of chain components such that $J^\tau(\cdot | x_{\text{pa}(\tau)})$ satisfies the pairwise Markov property, if $J^\tau(\cdot | x_{\text{pa}(\tau)})$ satisfies the intersection property, then it can be seen that the chain components are jointly independent using the global Markov property, since the chain components are not connected by paths.

Thus, the functional assignment $X_\tau = f_\tau(X_{\text{pa}(\tau)}, \epsilon_\tau)$ for the part τ can be decomposed into multiple functional assignments:

$$X_{\tau'_i} = f_{\tau'_i}(X_{\text{pa}(\tau)}, \epsilon_{\tau'_i}),$$

where $\tau'_i \in \{\tau'_1, \dots, \tau'_m\}$, with $\epsilon_\tau = (\epsilon_{\tau'_1}, \dots, \epsilon_{\tau'_m})$, where the constituent errors are jointly independent.

Having multiple chain components from a part does not affect the proof of Theorem 1. However, without loss of generality, we will consider structural equilibrium models such that, for each part, τ does not decompose w.r.t. the distribution $J^\tau(\cdot | x_{\text{pa}(\tau)})$. Thus we will assume that each part τ is a chain component in the corresponding graph \mathcal{G} . \diamond

If the corresponding graph \mathcal{G} is antierial, then the distribution P , assumed to be a compositional graphoid, induced from the structural equilibrium model is Markovian to \mathcal{G} .

Theorem 1 (Markov property for structural equilibrium models) *Let P be the joint distribution over the variables X_V induced from a structural equilibrium model and let the corresponding graph \mathcal{G} over the nodes V , as constructed in Algorithm 1, be antierial. If P is a compositional graphoid, then P is Markovian to \mathcal{G} .*

Throughout this work, we will assume structural equilibrium models that correspond to antierial graphs, via Algorithm 1. In addition to Definition 7, these models have an additional constraint: for any parts

$\tau'_1, \tau'_m \in \{\tau_1, \dots, \tau_n\}$, if there is a sequence of parts $\langle \tau'_1, \tau'_2, \dots, \tau'_{m-1}, \tau'_m \rangle$ such that τ'_i intersects $\text{pa}(\tau'_{i+1})$ for each consecutive parts τ'_i and τ'_{i+1} , then $\epsilon_{\tau'_1} \perp\!\!\!\perp \epsilon_{\tau'_m}$. Indeed, this condition can be graphically expressed as the lack of semi-directed paths between endpoints of a bidirected edge. See Section A.5 on why the antierial assumption is important for causal interpretability.

In the case where the corresponding graph is a chain graph, Lauritzen and Richardson (2002, Proposition 6) gives the Markov property for \mathcal{G} when viewing the chain graph as a DAG with chain components as nodes. Theorem 1 enables the consideration of conditional independencies involving *every* subset of nodes, addressing the remark from Dawid (2009) regarding the full extraction of conditional independencies from the chain graph.

When the parts of the structural equilibrium model are singletons, Algorithm 1 returns a graph of only directed and bidirected edges. When the errors in the structural equilibrium model are jointly independent, Algorithm 1 returns a chain graph. With the additional assumption that the induced distribution is a compositional graphoid, Theorem 1 extends the Markov property results in Sadeghi and Soo (2022, Theorem 27) for ancestral graphs and Lauritzen and Richardson (2002) for chain graphs.

Step 3 of Algorithm 1 connects either all or none of the nodes between the chain components τ and τ' with bidirected edges.

Definition 8 (Chain-connected graph) A graph \mathcal{G} is *chain-connected* if for all nodes i and j , we have

$$i \leftrightarrow j \Rightarrow i \leftrightarrow k \quad \text{for all } k \in \tau(j).$$

Thus, it can be seen that the corresponding graph \mathcal{G} is chain-connected. This can be interpreted as all nodes in the chain component τ sharing the same error ϵ_τ . Throughout this work, we will describe structural equilibrium models using chain-connected antierial graphs. Common graph classes such as DAGs, ancestral graphs and chain graphs are still a subclass of chain-connected antierial graphs.

Remark 5 In principle, Step 3 of Algorithm 1 can be modified to add bidirected edges based on conditional independencies of the induced joint distribution P , while still preserving the Markov property required. However, this approach is instead distributional, depending on the actual coupling of the errors, and no longer purely structural, depending only on the independencies of the errors, which allows for causal operations in an interpretable graphical manner. See also a similar argument on the importance of the antierial assumption on causal interpretability in Section A.5. \diamond

3.1. Interpreting the constructed graphical model \mathcal{G}

In Lauritzen and Richardson (2002), each chain component τ of a chain graph model is associated with a dynamical process, such as a Gibbs sampler (Geman and Geman, 1984), having a conditional equilibrium distribution given $x_{\text{pa}(\tau)}$, which we denote as $J^\tau(\cdot | x_{\text{pa}(\tau)})$. As suggested by the notation, given a structural equilibrium model, for every part τ , we will similarly associate the law $J^\tau(\cdot | x_{\text{pa}(\tau)})$ of $f_\tau(x_{\text{pa}(\tau)}, \epsilon_\tau)$ with the equilibrium distribution of the Gibbs sampler as follows.

Label the nodes in the chain component from 1 to $|\tau|$. Let $X_\tau^0 = x_\tau^0$ be some initial values and $m_0 = 1$ be the starting node of the Gibbs sampler, at every timestep t the values X_τ^t and node m_t are updated as follows:

$$\begin{aligned} m_t &= m_{t-1} + 1 \bmod |\tau|, \\ X_{\tau \setminus m_t}^t &= x_{\tau \setminus m_t}^{t-1}, \text{ and} \\ X_{m_t}^t &\sim J_{m_t}^\tau(\cdot | x_{\text{ne}(m_t)}^{t-1}; x_{\text{pa}(m_t)}). \end{aligned} \tag{5}$$

Remark 6 Given a structural equilibrium model, interpreting $J^\tau(\cdot | x_{\text{pa}(\tau)})$ as the equilibrium distribution of some dynamical process is only required to define sensible notions of interventions in Section 4. Observationally, it suffices to consider $J^\tau(\cdot | x_{\text{pa}(\tau)})$ only, since Theorem 1 is a statement on the observational joint distribution and therefore holds regardless of the exact dynamical process. \diamond

Despite ancestral graphs being closed under marginalisation and conditioning, we will discuss why interpretations based on marginalisation and conditioning of existing graph classes are not suitable for chain-connected ancestral graphs.

Marginalising chain graphs results in ancestral graphs (Sadeghi, 2016). Building on top of existing chain graph interpretations (Lauritzen and Richardson, 2002), one may be tempted to consider ancestral graphs as the marginal of a chain graph with latent variables, with bidirected edges $i \leftrightarrow j$ representing a latent variable between nodes i and j . However, Example 1 shows the problem with such an interpretation.

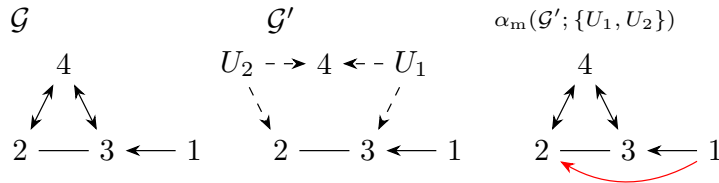


Fig. 2: Left: Chain-connected ancestral graph \mathcal{G} . Middle: Interpretation of bidirected edges $3 \leftrightarrow 4$ and $2 \leftrightarrow 4$ in \mathcal{G} as unobserved latent variables U_1 and U_2 respectively, from the chain graph \mathcal{G}' . Right: Graph $\alpha_m(\mathcal{G}'; \{U_1, U_2\})$ obtained by marginalising \mathcal{G}' over the latent variables U_1 and U_2 .

Example 1 (Problem with interpretations based on marginalisation) Consider Figure 2 and interpret the bidirected edges in the chain-connected ancestral graph \mathcal{G} as the existence of unobserved latent variables U_1 and U_2 , as shown in the chain graph \mathcal{G}' . Marginalising over U_1 and U_2 in \mathcal{G}' results in $\alpha_m(\mathcal{G}'; \{U_1, U_2\})$ which is not Markov equivalent to \mathcal{G} ; indeed, $1 \perp_{\mathcal{G}} 2 \mid 3$, but this separation does not hold in the marginalisation $\alpha_m(\mathcal{G}'; \{U_1, U_2\})$.

Similar issues with marginal chain graph models have been raised by Shpitser (2015) and were resolved using graphs containing undirected, directed, and bidirected edges. However, the directed edges in such graphs do not seem to have a clear interpretation (Shpitser, 2015, Section 2).

Similarly, conditioning ancestral graphs results in ancestral graphs (Sadeghi, 2016). Building on top of existing interpretations of ancestral graphs (Richardson and Spirtes, 2002; Sadeghi and Soo, 2022), it may also be tempting to interpret ancestral graphs as the conditional of ancestral graphs with selection variables, where the undirected edges $i - j$ is interpreted as conditioning on a selection bias variable between the nodes i and j from an ancestral graph. However, Example 2 shows a similar problem with such an interpretation.

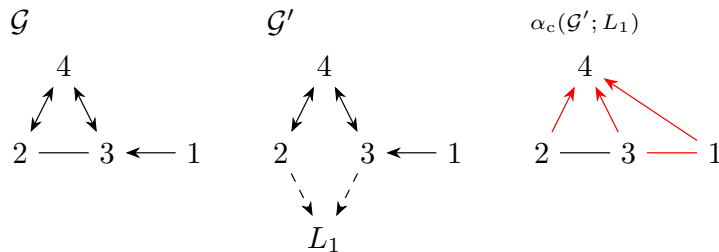


Fig. 3: Left: Chain-connected ancestral graph \mathcal{G} . Middle: Interpretation of the undirected edge $2 - 3$ as the selection bias variable L_1 from the ancestral graph \mathcal{G}' . Right: Graph $\alpha_c(\mathcal{G}'; L_1)$ obtained by conditioning \mathcal{G}' over the selection bias variable L_1 .

Example 2 (Problem with interpretations based on conditioning) Consider Figure 3 and interpret the undirected edge $2 - 3$ in the chain-connected arterial graph \mathcal{G} as the existence of selection variables L_1 , as shown in the ancestral graph \mathcal{G}' . Conditioning on L_1 in \mathcal{G}' results in $\alpha_c(\mathcal{G}'; L_1)$, which is not Markov equivalent to \mathcal{G} ; indeed, $1 \perp_{\mathcal{G}} 4$ but this separation does not hold in the conditional graph $\alpha_c(\mathcal{G}'; L_1)$.

3.2. Examples and simulations

To illustrate Theorem 1, we will simulate data from structural equilibrium models that correspond to the chain-connected arterial graphs in Figures 4, 5, and 6 in Python. Since the joint distribution in Theorem 1 is induced from the distributions over chain components $J^\tau(\cdot | x_{\text{pa}(\tau)})$, which we interpret as equilibrium of Gibbs samplers in (5), the simulation also allows us to test the validity of the Markov property of the structural equilibrium model when interpreted as Gibbs samplers in finite-time.

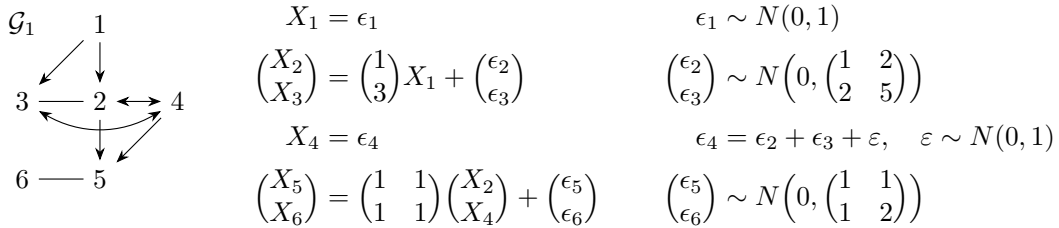


Fig. 4: Left: Corresponding chain-connected arterial graph \mathcal{G}_1 . Middle: Structural equilibrium model. Conditioning on 5, the distribution $J_6^{\{5,6\}}(\cdot | x_5; x_{\{2,4\}})$ does not depend on $x_{\{2,4\}}$, thus $\text{pa}(6) = \emptyset$. Right: Distribution and coupling of the error variables.

We will consider the structural equilibrium model which corresponds to the graph \mathcal{G}_1 in Figure 4. We sample 10000 data points directly from the structural equilibrium model (using the equilibrium distributions) and 1000 data points using a Gibbs sampler of the conditional normal distributions $J^{\{2,3\}}(\cdot | x_1)$ and $J^{\{5,6\}}(\cdot | x_2, x_4)$ with a burn-in of 10000 steps.

Using both sampled datasets, we perform a Fisher-Z test (using the `causal-learn` (Zheng et al., 2024) package) with a null hypothesis of pairwise conditional independence of the form $i \perp\!\!\!\perp j | \text{ant}(i, j)$ for every pair of nodes i and j . The Markov property w.r.t. the graph \mathcal{G}_1 would imply pairwise conditional independencies for some nodes i and j . The p-values for every pair of nodes are shown in Figure 17 in Section A.7.

Next, we consider the structural equilibrium model which corresponds to the graph \mathcal{G}_2 in Figure 5. Again, the p-values for the pairwise conditional independence tests are shown in Figure 18 in Section A.7.

We will use the structural equilibrium model which corresponds to the graph \mathcal{G}_3 in Figure 6.

The p-values for the pairwise independence tests are shown in Figure 19 in the Section A.7.

In Figure 19, high p-values indicate insufficient evidence for rejecting the null hypothesis in favour of the alternative hypothesis where $i \not\perp\!\!\!\perp j | \text{ant}(i, j)$, implying conditional independence. We see that the Fisher Z-test rejects the null hypothesis in a manner consistent with the conditional independencies implied by the Markov property of Theorem 1. Note that due to the higher dimensionality when sampling $\{3, 4, 5\}$, the p-values of the pairwise conditional independencies $5 \perp\!\!\!\perp 1 | \{2, 3, 4\}$ and $5 \perp\!\!\!\perp 3 | \{2, 1, 4\}$ are on the order of about 10^{-7} , while all the other returned p-values are close to 0.

4. Graphical Interventions of Structural Equilibrium Models

Given a structural equilibrium model with the corresponding graph \mathcal{G} , using the interpretation of a chain component τ of \mathcal{G} as the Gibbs sampler in (5), an intervention on a treatment set $C \subseteq V$ (to intervened values a_C) can be expressed through the following intervened Gibbs sampler by replacing the updating of

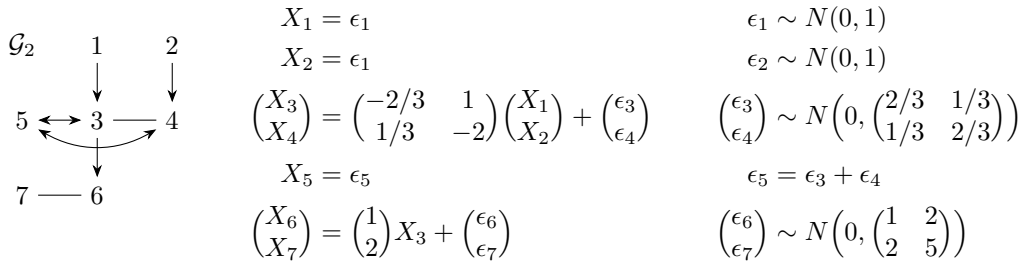


Fig. 5: Left: Corresponding chain-connected arterial graph \mathcal{G}_2 . Middle: Structural equilibrium model. Conditioning on 3, the distribution $J_4^{\{3,4\}}(\cdot | x_3; x_{\{1,2\}})$ depends on x_2 only, thus $\text{pa}(4) = 2$, similarly we have $\text{pa}(3) = 1$. Right: Distribution and coupling of the error variables.

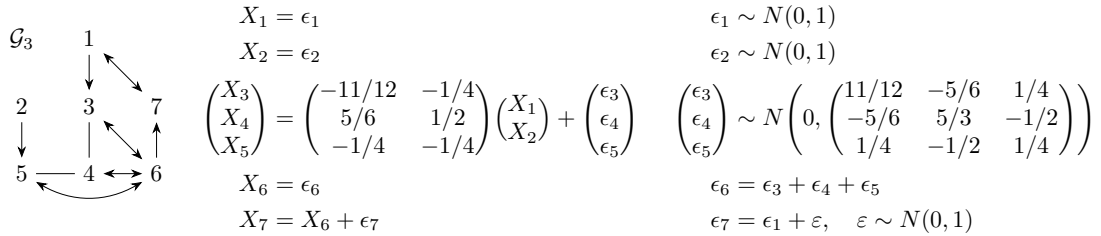


Fig. 6: Left: Corresponding Chain-connected arterial graph \mathcal{G}_1 . Middle: Structural equilibrium model. $3 \perp\!\!\!\perp 5$ holds for the distribution $J^{\{3,4,5\}}(\cdot | x_{\{2,4\}})$, thus 3 is not connected to 5. Conditioning on $\text{ne}(4)$, the distribution $J_4^{\{3,4,5\}}(\cdot | x_{\{3,5\}}; x_{\{1,2\}})$ does not depend on $x_{\{1,2\}}$, thus $\text{pa}(4) = \emptyset$. Likewise for $\text{pa}(3) = 1$ and $\text{pa}(5) = 2$. Right: Distribution and coupling of the error variables.

the treatment nodes in C with fixed assignments. This replacement results in the *intervened* Gibbs sampler as follows, expressed using the notation of the Gibbs sampler in (5):

$$\begin{aligned}
 & m_t = m_{t-1} + 1 \bmod |\tau|, \\
 & \text{if } m_t \in C, \\
 & \quad X_{\tau \setminus C}^t = x_{\tau \setminus C}^{t-1}, \text{ and} \\
 & \quad X_{\tau \cap C}^t = a_{\tau \cap C}, \\
 & \text{if } m_t \notin C, \\
 & \quad X_{\tau \setminus m_t}^t = x_{\tau \setminus m_t}^{t-1}, \text{ and} \\
 & \quad X_{m_t}^t \sim J_{m_t}^\tau(\cdot | x_{\text{ne}(m_t)}^{t-1}; x_{\text{pa}(m_t)}), \tag{6}
 \end{aligned}$$

with the conditional distribution $J_{m_t}^\tau(\cdot | x_{\text{ne}(m_t)}^{t-1}; x_{\text{pa}(m_t)})$ being the same in the Gibbs sampler (5) of the structural equilibrium model.

The resulting equilibrium distribution $J^{\tau, \text{do}(C)}(\cdot | x_{\text{pa}(\tau)})$ on the chain component τ is

$$J^{\tau, \text{do}(C)}(\cdot | x_{\text{pa}(\tau)}) = J_{\tau \setminus C}^{\tau}(\cdot | a_{\tau \cap C}; x_{\text{pa}(\tau)}) \delta_{\tau \cap C}(a_{\tau \cap C}), \quad (7)$$

where $J_{\tau \setminus C}^{\tau}(\cdot | a_{\tau \cap C}; x_{\text{pa}(\tau)})$ is the conditional distribution of the equilibrium distribution $J^{\tau}(\cdot | x_{\text{pa}(\tau)})$ of the pre-intervened Gibbs sampler (5) and $\delta_{\tau \cap C}(a_{\tau \cap C})$ is the delta function that takes the value 1 when $X_{\tau \cap C}$ takes the intervened values $a_{\tau \cap C}$; this is a local version of Lauritzen and Richardson (2002, Section 6.4, Equation 18).

From the distributions $J^{\tau, \text{do}(C)}(\cdot | x_{\text{pa}(\tau)})$, we define the resulting *intervened structural equilibrium model* by replacing the assignments for all chain components τ such that $\tau \cap C \neq \emptyset$ in the structural equilibrium model with

$$X_{\tau} = f_{\tau}^{\text{do}(C)}(X_{\text{pa}(\tau)}, \epsilon_{\tau}), \quad (8)$$

such that

- $f_{\tau}^{\text{do}(C)}(x_{\text{pa}(\tau)}, \epsilon_{\tau}) \sim J^{\tau, \text{do}(C)}(\cdot | x_{\text{pa}(\tau)})$, and
- the chain component errors $\epsilon_{\tau_1}, \dots, \epsilon_{\tau_n}$ have the same joint distribution as the errors in the observational structural equilibrium model (pre-intervention).

The intervened structural equilibrium model induces a new set of intervened random variables $X_V^{\text{do}(C)}$ with which we associate a joint interventional distribution $P^{\text{do}(C)}$.

Remark 7 Generally, in structural equilibrium models, the joint interventional distribution is not equivalent to the joint conditional distribution. However, this equivalence holds for the conditional distribution of the variable given its parents. This equivalence is compatible with the relationship in (7). \diamond

Remark 8 Lauritzen and Richardson (2002) also consider Langevin diffusions in lieu of Gibbs samplers. Given an observational distribution P , the interventional distribution $P^{\text{do}(C)}$ obtained from an intervened dynamical process using (8) depends on the dynamical process being considered.

A Gibbs sampler is chosen for this work as the dynamical process, since the resulting intervention can be expressed purely graphically (see Algorithm 2); the same cannot be said about other dynamical processes in Lauritzen and Richardson (2002) such as Langevin diffusions, for which the notion of intervention defined will depend on diffusion parameters.

Note that without assuming the dynamical process to be a Gibbs sampler, an equilibrium distribution may not exist after intervening the dynamical process. \diamond

4.1. Representing interventions graphically

Via a graphical operation (Algorithm 2) on the corresponding graph \mathcal{G} of the *observational* structural equilibrium model, we can describe the interventional distribution $P^{\text{do}(C)}$ after intervening on a treatment set C .

Algorithm 2 Intervening chain-connected arterial graphs

Input: chain-connected arterial graph \mathcal{G} , node subset $C \subseteq V$

Output: chain-connected arterial graph $\text{do}_C(\mathcal{G})$

For all $i \in C$,

- 1: for nodes j such that $i - j$, if $j \notin C$, then replace with $i \rightarrow j$; if $j \in C$, then remove edge $i - j$,
 - 2: remove all directed edges into i , and
 - 3: remove all bidirected edges $i \leftrightarrow j$.
-

Algorithm 2 first modifies undirected edges of nodes in the treatment set C and then removes directed and bidirected edges connected to C . See Figure 7 for an illustration of Algorithm 2.

When \mathcal{G} is a DAG, only Step 2 of Algorithm 2 is performed, and Algorithm 2 reduces to a standard graphical intervention for DAGs. Since interventions can be expressed distributionally as a truncated

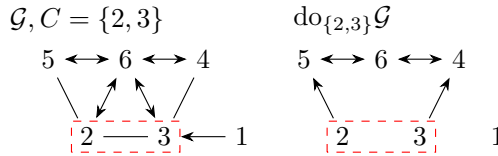


Fig. 7: Left: Input chain-connected arterial graph \mathcal{G} and treatment set $C = \{2, 3\}$. Right: Output $\text{do}_C(\mathcal{G})$ after removing bidirected and directed edges into C .

factorisation of the observational distribution, the interventional distribution is Markovian to $\text{do}_C(\mathcal{G})$ (Spirtes et al., 2000, Theorem 3.6).

Theorem 2 similarly describes $P^{\text{do}(C)}$ from structural equilibrium models using the intervened (arterial) graph $\text{do}_C(\mathcal{G})$.

Theorem 2 (Markov property for interventions) *Let $P^{\text{do}(C)}$ be the interventional distribution (from intervening on a treatment set C) induced from a structural equilibrium model corresponding to the chain-connected arterial graph \mathcal{G} . If $P^{\text{do}(C)}$ is a compositional graphoid, then $P^{\text{do}(C)}$ is Markovian to $\text{do}_C(\mathcal{G})$.*

Note that the intervened structural equilibrium model is still a structural equilibrium model. Using the relationship in (7), Algorithm 2 constructs the corresponding graph $\text{do}_C(\mathcal{G})$ from the observational graph \mathcal{G} . Theorem 1 is used to show Theorem 2.

Remark 9 (The splitting of chain components when intervening can be dealt with similarly as in Remark 4.) *In Figure 7, the chain component $\{2, 3, 4, 5\}$ in \mathcal{G} is split into multiple chain components in $\text{do}_C(\mathcal{G})$. In general, given a chain component τ in \mathcal{G} , the nodes in $\tau \setminus C$ can be partitioned into different chain components τ_i^{do} in $\text{do}_C(\mathcal{G})$, such that $\bigcup_{i=1}^n \tau_i^{\text{do}} = \tau \setminus C$.*

As argued in Remark 4 (by the global Markov property of the constructed τ), these components τ_i^{do} are jointly independent given $a_{\tau \cap C}$, then we can decompose the functional assignment $X_\tau = f_\tau^{\text{do}(C)}(X_{\text{pa}(\tau)}, \epsilon_\tau)$ in (8) into

$$X_{\tau \cap C} = a_{\tau \cap C}, \text{ and}$$

$$X_{\tau_i^{\text{do}}} = f_{\tau_i^{\text{do}}}(X_{\text{pa}(\tau)}, X_{\tau \cap C}, \epsilon_{\tau_i^{\text{do}}}),$$

for each $\tau_i^{\text{do}} \in \{\tau_1^{\text{do}}, \dots, \tau_n^{\text{do}}\}$, such that $\epsilon_\tau = (\epsilon_{\tau_1^{\text{do}}}, \dots, \epsilon_{\tau_n^{\text{do}}})$ where each $\epsilon_{\tau_i^{\text{do}}}$ are jointly independent and $f_{\tau_i^{\text{do}}}(x_{\text{pa}(\tau)}, x_{\tau \cap C}, \epsilon_{\tau_i^{\text{do}}}) \sim J_{\tau_i^{\text{do}}}^\tau(\cdot | a_{\tau \cap C}; x_{\text{pa}(\tau)})$. \diamond

4.2. Counterfactual Interpretations

In line with counterfactual interpretations in (Pearl, 2009, Chapter 7); Balke and Pearl (1994), after intervening on a treatment set C , using the structural equilibrium model, a coupling between observational variables X_V and intervened variables $X_V^{\text{do}(C)}$ is induced via common errors. Here, we describe this coupling, and provide a graphical representation of this coupling.

Consider a structural equilibrium model with the corresponding chain-connected arterial graph \mathcal{G} . Given some chain component τ in \mathcal{G} , intervention on a treatment set $C \subseteq V$ by setting $X_C = a_C$ for some fixed value a_C induces a coupling between observational variables X_τ and intervened variables $X_\tau^{\text{do}(C)}$ via the common error ϵ_τ of the functional assignments of the combined structural equilibrium model, shown as follows:

$$\begin{aligned}
X_\tau &= f_\tau(X_{\text{pa}(\tau)}, \epsilon_\tau), \text{ and} \\
X_\tau^{\text{do}(C)} &= f_\tau^{\text{do}(C)}(X_{\text{pa}(\tau)}^{\text{do}(C)}, \epsilon_\tau), \text{ if } \tau \cap C \neq \emptyset \\
X_\tau^{\text{do}(C)} &= f_\tau(X_{\text{pa}(\tau)}^{\text{do}(C)}, \epsilon_\tau), \text{ if } \tau \cap C = \emptyset,
\end{aligned} \tag{9}$$

where $f_\tau^{\text{do}(C)}$ is the intervened function from (8).

4.2.1. Representing the coupling graphically

Given an antieral graph \mathcal{G} , and a node subset $C \subseteq V$, we apply the graphical operation introduced in Algorithm 3, and denote the resulting graph as $\phi(\mathcal{G}; C)$. See Figure 8 for an illustration of Algorithm 3.

Algorithm 3 Counterfactual Graph, ϕ

Input: antieral graph \mathcal{G} , node subset $C \subseteq V$

Output: graph $\phi(\mathcal{G}; C)$

- 1: Reproduce \mathcal{G} and construct $\text{do}_C(\mathcal{G})$, relabelling all the nodes i in $\text{do}_C(\mathcal{G})$ as $i^{\text{do}(C)}$.
 - 2: For nodes $i \notin C$ in \mathcal{G} such that $C \cap \text{ant}(i) = \emptyset$, remove $i^{\text{do}(C)}$ and replace edges between $i^{\text{do}(C)}$ and nodes of the form $j^{\text{do}(C)}$ with the same edge between i and $j^{\text{do}(C)}$.
 - 3: Add bidirected edges based on Table 1.
-

If in \mathcal{G}	Then
1. $i \notin C$	add $i^{\text{do}(C)} \leftrightarrow i$
2. $i \leftrightarrow j$ and $i \notin C$	add $i^{\text{do}(C)} \leftrightarrow j$
3. $j \in \tau(i)$ and $i \notin C$	add $i^{\text{do}(C)} \leftrightarrow j$

Table 1. Bidirected edges between relabelled nodes in $\text{do}_C(\mathcal{G})$ and nodes in \mathcal{G} , based on conditions on the corresponding nodes in \mathcal{G} .

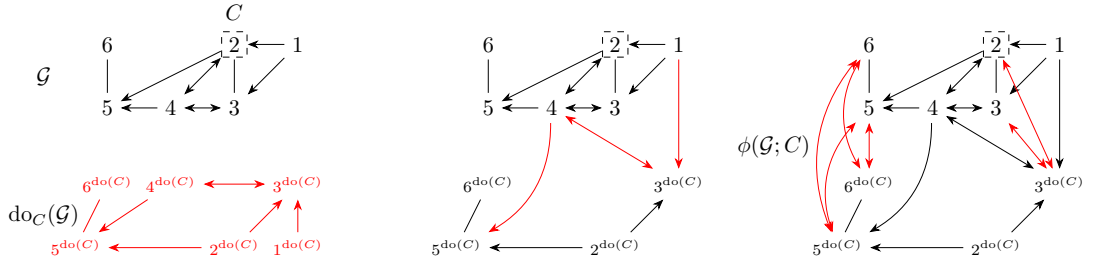


Fig. 8: Consider the input antieral graph \mathcal{G} with $C = 2$. Left: Algorithm 3 first creates $\text{do}_C(\mathcal{G})$ using Algorithm 2 with the nodes relabelled alongside input graph \mathcal{G} . Middle: Algorithm 3 merges nodes in \mathcal{G} and $\text{do}_C(\mathcal{G})$. Right: Algorithm 3 then introduces bidirected edges between \mathcal{G} and $\text{do}_C(\mathcal{G})$ based on Table 1 to obtain $\phi(\mathcal{G}; 2)$.

Algorithm 3 first introduces all the intervened variables $X^{\text{do}(C)}$ alongside the observational variables X_V . For a node i in \mathcal{G} such that there does not exist a semi-directed path in \mathcal{G} from treatment set C to node i , the observational variable X_i is equal to $X_i^{\text{do}(C)}$. Step 2 of Algorithm 3 accounts for this equality by merging all such observational variables X_i and intervened variables $X_i^{\text{do}(C)}$, represented by the nodes i

and $i^{\text{do}(C)}$, respectively, into the node i . The edges between $i^{\text{do}(C)}$ and the other nodes $j^{\text{do}(C)}$ are preserved as the same edge between i and $j^{\text{do}(C)}$.

Table 1 introduces bidirected edges between nodes $i^{\text{do}(C)}$ and nodes j in \mathcal{G} to capture the dependence of the chain component errors $\epsilon_{\tau(i)}$ and $\epsilon_{\tau(j)}$ that are shared between the corresponding variables $X_{\tau(i)}^{\text{do}(C)}$ and X_j (since errors are shared in (9)), when the corresponding node i in \mathcal{G} is not in treatment set C .

In the case of DAGs, Algorithm 3 reduces to the construction of counterfactual graphs from Shpitser and Pearl (2007), where the common errors are marginalised over.

Using the structural equilibrium model (corresponding to graph \mathcal{G}), the coupling between observational and intervened variables is described via $\phi(\mathcal{G}; C)$. Let node $i^{\text{do}(C)}$ in graph $\phi(\mathcal{G}; C)$ represent $X_i^{\text{do}(C)}$.

Theorem 3 (Markov property of the counterfactual interpretation) *Let the observational random variables X_V be induced from a structural equilibrium model corresponding to the chain-connected arterial graph \mathcal{G} . Let the combined structural equilibrium model in (9) induce the joint distribution P^* be the joint distribution over X_V and $X_V^{\text{do}(C)}$. If P^* is a compositional graphoid, then P^* is Markovian to $\phi(\mathcal{G}; C)$.*

Theorem 3 is shown by observing that the combined structural equilibrium model (9) is another structural equilibrium model, with the corresponding graph $\phi(\mathcal{G}; C)$. Theorem 1 is used to show Theorem 3.

Note that the nodes merged in Step 2 of Algorithm 3 correspond to counterfactual variables that are equivalent to observational variables, that is, $X_i^{\text{do}(C)} = X_i$; thus Theorem 3 describes the full joint distribution of observational and intervened variables. This merging step also avoids certain deterministic relationships between nodes in the graph $\phi(\mathcal{G}; C)$, which can lead to violations of the faithfulness condition, leading to erroneous results as highlighted in Richardson and Robins (2013, Figure 15). However, errors are still shared between observational and intervened variables, as indicated by the bidirected edge $3 \leftrightarrow 3^{\text{do}(C)}$ in $\phi(\mathcal{G}; C)$ of Figure 8, which can potentially lead to violations of faithfulness. This motivates an alternative graphical representation inspired by single-world intervention graphs (SWIGs) from Richardson and Robins (2013).

4.2.2. Single-world interpretation

Using Algorithm 3, the constructed $\phi(\mathcal{G}; C)$ describes the relationship of both observational and interventional versions of the same variable entailed by the combined structural equilibrium model (9), represented by having both $i^{\text{do}(C)}$ and i as nodes in the same graph.

However, outside of settings where one has a full description of the underlying data generating process (in our case, the structural equilibrium model), causal inference has the fundamental problem where only *one* version of the same variable is observed (Holland, 1986). To accommodate this issue, we will also graphically represent the single-world counterfactual distribution consisting of only one version (observational or intervened) of each variable that is not in the treatment set C , in line with Richardson and Robins (2013).

Let the *posterior* of C in the observational graph \mathcal{G} be given by

$$\text{po}(C) = \{j \notin C : \text{there is a semi-directed path from } i \in C \text{ to } j \text{ in } \mathcal{G}\}.$$

By marginalising the counterfactual graph $\phi(\mathcal{G}; C)$ using α_m with $M = \text{po}(C)$, we obtain $\alpha_m(\phi(\mathcal{G}; C); \text{po}(C))$, which we call $\phi'(\mathcal{G}; C)$; see Figure 9 for an example.

Based on Theorem 3, we have the following.

Proposition 4 (Markov property of the single-world interpretation) *Let the combined structural equilibrium model in (9) induce P^* , the joint distribution over X_V and $X_V^{\text{do}(C)}$, and let P^* be a compositional graphoid. Let P_{sub}^* be the distribution of variables in $\phi'(\mathcal{G}; C)$. The distribution P_{sub}^* is Markovian to $\phi'(\mathcal{G}; C)$.*

When \mathcal{G} is a DAG, marginalising $\text{po}(C)$ from $\phi(\mathcal{G}; C)$ is equivalent to taking the subgraph over the remaining nodes not in $\text{po}(C)$, since there are no nodes in $j \in \text{po}(C)$ and $k \notin \text{po}(C)$ such that $j \rightarrow k$. Observe that SWIGs (Richardson and Robins, 2013) relabel the descendants i of C as $i^{\text{do}(C)}$, and nodes

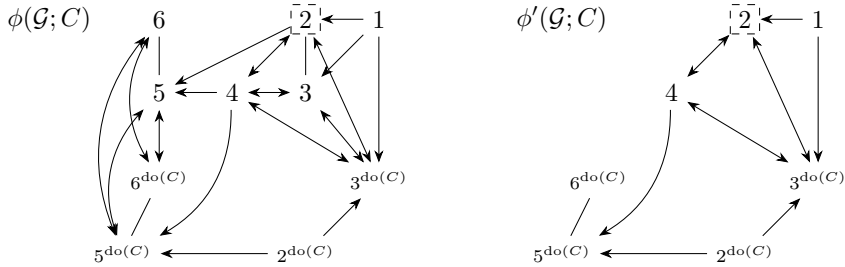


Fig. 9: Left: $C = 2$ and $\text{po}(C) = \{3, 5, 6\}$. Right: The single-world anterial interventional graph (SWAIG) $\phi'(\mathcal{G}; C)$ obtained by marginalising $\text{po}(C)$ from $\phi(\mathcal{G}; C)$.

$j \in C$ get split into $j^{\text{do}(C \setminus j)}$ and $j^{\text{do}(C)}$. Thus, $\phi'(\mathcal{G}; C)$ contains all variables in the SWIG *except* the intervened variables of the form $X_i^{\text{do}(B)}$ where $B \subseteq C$.

In the case when the treatment set $C = i$ is a singleton, it can be seen that the resulting graph $\phi'(\mathcal{G}; C)$ contains *all* the variables in the SWIG. Thus, we will refer to $\phi'(\mathcal{G}; C)$, in the case when \mathcal{G} is a general anterial graph, as a *single-world anterial interventional graph* (SWAIG). Proposition 4 then implies the Markov property of SWIGs with the additional condition that the joint distribution over observational and intervened variables is a compositional graphoid.

In Figure 9, note that there are no more bidirected edges between observational nodes i and $j^{\text{do}(C)}$ in $\phi'(\mathcal{G}; C)$. This is because we consider only one version (observational or intervened) of each variable, hence common shared errors, and thus faithfulness violations, are avoided. However, note that, by including fewer variables, $\phi'(\mathcal{G}; C)$ implies less conditional independencies than $\phi(\mathcal{G}; C)$.

Remark 10 (Taking into account of all nodes in the SWIG) *When \mathcal{G} is a DAG, nodes of the form $j^{\text{do}(C \setminus j)}$ can be included by extending the construction of Algorithm 3 based on parallel-world graphs (Avin et al., 2005); see section A.6 to see how SWIGs are subgraphs of counterfactual graphs.* \diamond

5. Confounder Selection with Constraints

The expression of common causal estimands such as the CATE and ETT in terms of the observational distribution depends on the *consistency* condition (Hernan and Robins, 2020, Page 4) and the unconfoundedness assumption (3), with the consistency condition being satisfied when intervening structural equilibrium models. Since structural equilibrium models induce a joint distribution over observational and intervened variables via common errors based on (9), the unconfoundedness assumption, and thus the notion of adjustment sets are well-defined.

Thus, we will consider the problem of selecting a minimal adjustment set S for the confounding of treatment variable X_C on outcome variable X_O subject to the following constraints L and U :

$$L \subseteq S \subseteq U, \quad (10)$$

where L and U are fixed set constraints.

These constraints may arise from some covariates that have to be excluded from S due to the economic and ethical costs of data collection, or covariates L that should be included in S such as prognostic variables following regulatory recommendations in adjusting for covariates from agencies like the FDA or EMA (U.S. Food and Drug Administration, 2023, Section III).

We assume we are given an anterial graph \mathcal{G}^* over the nodes V^* such that the joint distribution of $X_O^{\text{do}(C)}$, X_C , X_U , (and potentially other nuisance variables) is Markovian to \mathcal{G}^* . We also assume that the treatment set C and outcome set O are singletons, which we emphasise using the notation c and o . In the

case of a structural equilibrium model corresponding to a chain-connected antieral graph \mathcal{G} that induces the distribution P^* over X_V and $X_V^{\text{do}(C)}$, Theorem 3 and Proposition 4 imply that the counterfactual graph $\phi(\mathcal{G}; c)$ and the SWAIG $\phi'(\mathcal{G}; c)$ are examples of the antieral graph \mathcal{G}^* .

In practice, the graph $\phi(\mathcal{G}; c)$, and thus $\phi'(\mathcal{G}; c)$ after applying α_m to $\phi(\mathcal{G}; c)$, can be obtained by applying Algorithm 3 to the output of causal discovery algorithms that return an antieral graph \mathcal{G} from an input observational distribution P —these algorithms have been introduced by Meek and Sadeghi (2026).

The assumption (3) that the set S has to satisfy can then be expressed as a graphical separation of the graph \mathcal{G}^* . In the case when \mathcal{G}^* is a maximal ancestral graph, standard approaches such as from van der Zander et al. (2019) can then be applied to obtain S .

When \mathcal{G}^* is a general antieral graph, we present the element-wise procedure in Algorithm 4, taking the graph \mathcal{G}^* and the nodes $o^{\text{do}(c)}$ and c representing $X_o^{\text{do}(c)}$ and X_c , respectively, as inputs to return such a set S .

Algorithm 4 Constrained Confounder Selection

Input: antieral graph \mathcal{G}^* , nodes $o^{\text{do}(c)}, c \in V^*$, node subsets $L, U \subseteq V^*$ (not containing c and $o^{\text{do}(c)}$)

Output: set of nodes S

- 1: Obtain $\alpha_m(\alpha_c(\mathcal{G}^*; L); V^* \setminus (U \cup \{c, o^{\text{do}(c)}\}))$, call this \mathcal{G}_0^* .
 - 2: Maximise \mathcal{G}_0^* , by obtaining $\max(\mathcal{G}_0^*)$.
 - 3: **if** c is adjacent to $o^{\text{do}(c)}$ in $\max(\mathcal{G}_0^*)$ **then**
 - 4: **return** no feasible set.
 - 5: **else**
 - 6: Let $n = 0$ and $S = U$.
 - 7: **repeat until no such node**
 - 8: Select a node $i \in S \setminus L$ such that c and $o^{\text{do}(c)}$ are not adjacent in $\max(\mathcal{G}_{n+1}^*)$, where $\mathcal{G}_{n+1}^* = \alpha_m(\mathcal{G}_n^*; i)$.
 - 9: $S \leftarrow S \setminus i$.
 - 10: $n \leftarrow n + 1$.
 - 11: **return** S .
 - 12: **end if**
-

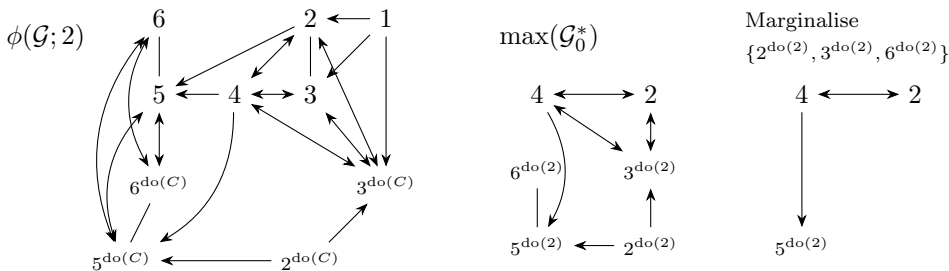


Fig. 10: Left: Graph $\phi(\mathcal{G}; 2)$ from Figure 8 is used as the input \mathcal{G}^* for Algorithm 4, with $L = 1$ and $U = V^* \setminus \{2, 3, 5, 6, 5^{\text{do}(2)}\}$, c and $o^{\text{do}(c)}$ being nodes 2 and $5^{\text{do}(2)}$ respectively. Middle: Graph $\max(\mathcal{G}_0^*)$ obtained after conditioning on L marginalising $V^* \setminus (U \cup \{c, o^{\text{do}(c)}\})$ and maximising. The feasibility check passes since 2 is not adjacent $5^{\text{do}(2)}$ in $\max(\mathcal{G}_0^*)$. Right: Graph after Algorithm 4 selects $\{2^{\text{do}(2)}, 3^{\text{do}(2)}, 6^{\text{do}(2)}\}$ to marginalise and maximise. Since further marginalising 4 would introduce edge $2 \leftrightarrow 5^{\text{do}(2)}$, the algorithm terminates and returns $\{1, 4\}$ as S .

Figure 10 illustrates how Algorithm 4 works. After marginalising the nodes not in $U \cup \{c, o^{\text{do}(c)}\}$ and conditioning on the nodes in L (using operations α_m and α_c from Section 2) to obtain \mathcal{G}_0^* , Algorithm 4

checks $\max(\mathcal{G}_0^*)$ to determine if there is an adjustment set S that satisfies (10). Algorithm 4 then removes nodes i from the upper set constraint U in a way that ensures, after removal, the existence of an adjustment set S where $L \subseteq S \subseteq U \setminus i$. This removal is iteratively applied to the upper bound until no nodes can be removed and the remaining upper bound is returned as S .

The general set-up of Algorithm 4, depending on the constraints L and U , allows for the inclusion of intervened variables in the adjustment set S . When S contains intervened variables, the obtained identification formula for causal estimands then contains terms from the interventional distribution and is not identifiable observationally. By excluding all the intervened variables from the set constraint U in Algorithm 4, only observational variables are allowed in the adjustment set S . We will not enforce this constraint, since there are cases such as sequential exchangeability in Hernan and Robins (2020, Section 19.5) where S contains intervened variables.

Note that after obtaining $\max(\mathcal{G}_0^*)$, if c is not adjacent to $o^{\text{do}(c)}$, Algorithm 4 can in principle return the set $L \cup \text{ant}(\{c, o^{\text{do}(c)}\})$ in $\max(\mathcal{G}_0^*)$ as S and terminate. Since nodes in $\max(\mathcal{G}_0^*)$ (that are not c and $o^{\text{do}(c)}$) are contained in U , the returned S would also satisfy $S \subseteq U$. However, in general, this does not lead to a *minimal* adjustment set. Consider $\max(\mathcal{G}_0^*)$ in Figure 10, since $L \cup 4$ is an adjustment set such that $L \cup 4 \subseteq L \cup \text{ant}(\{2, 5^{\text{do}(2)}\})$, it can be seen that $L \cup \text{ant}(\{2, 5^{\text{do}(2)}\})$ is not minimal. Similarly, $L \cup \text{pa}(\{c, o^{\text{do}(c)}\})$ in $\max(\mathcal{G}_0^*)$ is not minimal.

Theorem 5 (Correctness of Algorithm 4) *Let \mathcal{G}^* and the single nodes c and $o^{\text{do}(c)}$ be the inputs of Algorithm 4 and let the joint distribution of $X_o^{\text{do}(c)}$, X_c , X_U , (and potentially other nuisance variables) be Markovian to the anterial graph \mathcal{G}^* . When Algorithm 4 returns a set S , the set S is an adjustment set that satisfies $L \subseteq S \subseteq U$.*

Furthermore, let the joint distribution of $X_o^{\text{do}(c)}$, X_c , X_U , (and potentially other nuisance variables) be faithful to \mathcal{G}^ . It then holds that S is minimal and if Algorithm 4 returns no feasible set, then there does not exist an adjustment set S that satisfies $L \subseteq S \subseteq U$.*

Theorem 5 states that if we have access to an anterial graph \mathcal{G}^* (e.g. $\phi(\mathcal{G}; c)$) to which the distribution over a set of variables that contain the observational and intervened variable of interest is Markovian to, when Algorithm 4 returns a set S , this set is an adjustment set S that satisfies the constraint $L \subseteq S \subseteq U$. Furthermore, if this distribution is faithful to \mathcal{G}^* , then we can determine the existence of such a set S via the feasibility check of Algorithm 4, and that the returned adjustment set S is minimal.

Remark 11 (Faithfulness and confounder selection) *Note that the unconfoundedness assumption (3), and thus the notion of an adjustment set, does not refer to a graph and is purely probabilistic. Algorithm 4 determines the existence of a graphical separation set and finds a minimal graphical separation set in \mathcal{G}^* . The graphical separation sets correspond to the adjustment sets only when \mathcal{G}^* is a faithful graph. \diamond*

Note that in general, the maximising operation, \max , is required for Algorithm 4, even if we assume maximality of the input graph \mathcal{G}^* . As shown in Figure 11, a DAG which is always maximal can result in a non-maximal ancestral graph when marginalised (using α_m) causing the feasibility check using \mathcal{G}_0^* to be inaccurate.

To select an adjustment set S such that $L \subseteq S \subseteq U$ for arbitrary set constraints L and U , conventional approaches typically enumerate the adjustment sets efficiently (van der Zander et al., 2019) and implement the constraints post-hoc. By representing $X_o^{\text{do}(c)}$ and X_c in a Markovian graph \mathcal{G}^* (such as $\phi(\mathcal{G}; c)$ or $\phi'(\mathcal{G}; c)$, obtained from the observational graph \mathcal{G}), when \mathcal{G}^* is a maximal ancestral graph, efficient approaches for identifying sets satisfying graphical separations such as from van der Zander et al. (2019) can be used to select S . When \mathcal{G}^* is a general anterial graph, Algorithm 4 avoids constructing unfeasible adjustment sets by incorporating the constraints directly into the algorithm, and proceeds in an element-wise manner to select nodes to construct the minimal adjustment set.

An implementation of Algorithm 4, using the R package `ggm` (Marchetti et al., 2025) (developed for ancestral graphs) is hosted online: Teh (2026).

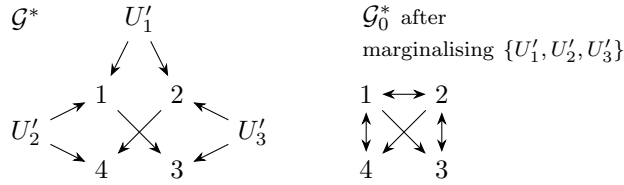


Fig. 11: Left: Input anterial graph \mathcal{G}^* to algorithm 4, with $L = \emptyset$, $U = \{1, 2, 3, 4\}$, and nodes C and $O^{\text{do}(C)}$ being 3 and 4. Note that \mathcal{G}^* is a DAG and is thus maximal. Right: Graph \mathcal{G}_0^* after marginalising over $\{U'_1, U'_2, U'_3\}$ in Algorithm 4 without maximising. We see that despite the absence of edges between nodes 3 and 4, there doesn't exist a set $S \subseteq \{1, 2, 3, 4\}$ such that $3 \perp_{\mathcal{G}^*} 4 \mid S$.

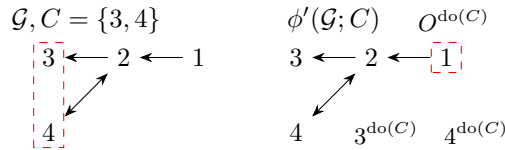


Fig. 12: Left: Anterial graph \mathcal{G} . Right: $\phi'(\mathcal{G}; C)$ with $O^{\text{do}(C)} = 1^{\text{do}(C)} = 1$ and $C = \{3, 4\}$.

Remark 12 (When C and $O^{\text{do}(C)}$ are node subsets) *Note that the formulation of Algorithm 4 requires the input C and $O^{\text{do}(C)}$ to be nodes. Consider the SWAIG $\phi'(\mathcal{G}; C)$ in Figure 12; here C is a two-element set. It is not difficult to see that there does not exist a node subset S in $\phi'(\mathcal{G}; C)$ such that $C \perp_{\phi'(\mathcal{G}; C)} O^{\text{do}(C)} \mid S$. Thus, in the case when the distribution over the nodes in $\phi'(\mathcal{G}; C)$ is faithful to $\phi'(\mathcal{G}; C)$, the absence of edges between C and $O^{\text{do}(C)}$ is not sufficient for the existence of an adjustment set, which is required for Algorithm 4.*

However, note that the converse is true, that is, presence of edges between subsets C and $O^{\text{do}(C)}$ implies the absence of an adjustment set. Thus, Algorithm 4 is still sound, but not complete, in detecting when there are no feasible adjustment sets. \diamond

6. Conclusion and Future Work

We provide graphical models for structural equilibrium models (Definition 7), a generalisation of structural causal models, which also accounts for both equilibrium relationships and confounding. Given a structural equilibrium model, our graphical model is obtained using Algorithm 1, and is based on anterial graphs. This generalises existing causal graphical models based on chain graphs (Lauritzen and Richardson, 2002), ancestral graphs (Richardson and Spirtes, 2002; Sadeghi and Soo, 2022), and thus DAGs.

Following Lauritzen and Richardson (2002), we use Gibbs samplers as the underlying dynamical processes to describe interventions on a treatment set C for structural equilibrium models. Using our anterial graphical model \mathcal{G} of the structural equilibrium model, these interventions can be represented graphically as $\text{do}_C(\mathcal{G})$ (using Algorithm 2). Our anterial graphical model \mathcal{G} also allows for the joint representation of observational and intervened variables in a single graph, as either $\phi(\mathcal{G}; C)$ (via Algorithm 3) or $\phi'(\mathcal{G}; C)$ (by marginalising $\phi(\mathcal{G}; C)$). The counterfactual graph $\phi(\mathcal{G}; C)$ implies more counterfactual conditional independencies at the cost of potentially violating faithfulness, leading to errors similar to Figure 15 of Richardson and Robins (2013); the single-world interventional anterial graph $\phi'(\mathcal{G}; C)$ avoids deterministic relationships *and* common shared errors that lead to faithfulness violations, at the cost of encoding fewer conditional independencies.

Our arterial graphical model \mathcal{G} is causally interpretable since interventions on the graphical model can be performed by only modifying and deleting edges directly adjacent to nodes in the treatment set C . Due to this interpretability, algorithms involving interventions (Algorithms 2 and 3) depend only on the corresponding observational graph \mathcal{G} and do not depend on the exact coupling of the error variables in the structural equilibrium model.

We also provided an element-wise procedure to select an adjustment set S subject to $L \subseteq S \subseteq U$ with prescribed set constraints L and U (Algorithm 4). This provably returns the minimal adjustment set under conditions such as when the representation $\phi'(\mathcal{G}; C)$ introduced is faithful. Unlike conventional approaches, our method is valid for arterial graphs and avoids constructing unfeasible sets during the algorithm.

Theorems 1, 2, and 3 depend on the corresponding distributions being compositional graphoids, which is an assumption that is automatically made when one considers faithfulness (Sadeghi, 2017). Analogous to DAGs, chain graphs and ancestral graphs, the compositional graphoid condition can potentially be relaxed by defining a new notion of a local Markov property for the class of arterial graphs, which implies the Markov property without any strong further conditions.

We also note that in Algorithm 4, after checking for feasibility, only the marginalisation operation α_m is used iteratively. However, allowing the conditioning operation α_c to be used alongside α_m may improve the algorithm. Consider Figure 10, the minimal adjustment set $L \cup 4$ can be selected in just 2 steps by applying the marginalising operation α_m and the conditioning operation α_c to the middle graph of Figure 10 and maximising to obtain the graph in Figure 13. However, in general, conditioning may introduce unnecessary nodes into S , resulting in a S that is no longer minimal. Thus, speeding up Algorithm 4 by allowing for both α_m and α_c operations, while ensuring the minimality of the selected S is a subject of future interest.

In Section 4.2, we focused on counterfactual conditional independencies that relate observational and interventional variables where the intervened value is fixed, such as the unconfoundedness assumption (3). Extending this framework to capture more general counterfactual assumptions involving multiple intervention values is an important direction for future work. A potential approach is to use the “templates,” proposed by Richardson and Robins (2013), to systematically handle different intervened values.



Fig. 13: Graph obtained after marginalising $\{3^{do(2)}\}$, conditioning on 4 and maximising the middle graph $\max(\mathcal{G}_0^*)$ from Figure 10. Since there is no path from 2 to $5^{do(2)}$, it is clear that $2 \perp 5^{do(2)} \mid L \cup 4 = \{1, 4\}$, and $L \cup 4$ can be returned as a minimal adjustment set.

As can be seen in Remark 12, Algorithm 4 is only sound, but not complete, in detecting the absence of feasible adjustment sets when the inputs C and $O^{do(C)}$ are subset of nodes. Thus, extending Algorithm 4 to the multivariate setting where C and $O^{do(C)}$ are subsets of nodes remains to be investigated.

7. Acknowledgments

We thank Christopher Meek and Thomas Richardson for their insightful remarks and advice.

A. Appendix and Proofs

A.1. Proof of Theorem 1

We will use the following from Lauritzen and Sadeghi (2018) and Sadeghi and Soo (2022) to show Theorem 1.

Definition 9 (Chain mixed graph (Lauritzen and Sadeghi, 2018)) A chain mixed graph \mathcal{G} over a set of nodes V , is a graph which may contain directed, undirected, and bidirected edges, such that there does not exist semi-directed cycles in \mathcal{G} .

Anterial graphs are thus a subclass of chain mixed graphs where Item 1 of Definition 1 does not have to hold. Analogous to inducing paths in an ancestral graph, the notion of a *primitive inducing path* will be used to characterise the maximality of chain mixed graphs.

Definition 10 (Primitive inducing path) A primitive inducing path connecting the nodes i and j is a path $\pi = \langle i, q_1, \dots, q_n, j \rangle$ such that:

- $q_1, \dots, q_n \in \text{ant}(i, j)$,
- the edges between subsequent nodes q_1, \dots, q_n in π are either bidirected or undirected, and
- the edge between i and q_1 is either bidirected or $i \rightarrow q_1$, and the edge between j and q_n is either bidirected or $j \rightarrow q_n$.

We will use the notation $i \not\sim_p j$ to denote that the nodes i and j are not connected by a primitive inducing path. We will use the following version of Lauritzen and Sadeghi (2018) for our proof.

Proposition 6 ((Lauritzen and Sadeghi, 2018)) *A chain mixed graph \mathcal{G} is maximised by adding edges between non-adjacent nodes that are connected by a primitive inducing path. Call the resulting maximal graph $\text{max}(\mathcal{G})$. Furthermore, the anterior of \mathcal{G} is preserved; that is, $\text{ant}(i)$ in \mathcal{G} is the same as $\text{ant}(i)$ in $\text{max}(\mathcal{G})$, for every node i .*

Definition 11 (Pairwise Markov property (Lauritzen and Sadeghi, 2018)) The distribution P satisfies the pairwise Markov property w.r.t. the chain mixed graph \mathcal{G} if for nodes i and j , we have

$$i \text{ not adjacent to } j \text{ in } \mathcal{G} \Rightarrow i \perp\!\!\!\perp j \mid \text{ant}(i, j). \quad (11)$$

Proposition 7 (Theorem 4 (Lauritzen and Sadeghi, 2018)) *Let \mathcal{G} be a maximal chain mixed graph, and the distribution P be a compositional graphoid. The following equivalence holds.*

$$P \text{ satisfies the pairwise Markov property w.r.t. } \mathcal{G} \iff P \text{ is Markovian to } \mathcal{G}.$$

When \mathcal{G} is not maximal, we have the following version of Proposition 7.

Proposition 8 (Proposition 7 for non-maximal \mathcal{G}) *Let \mathcal{G} be a chain mixed graph, and the distribution P be a compositional graphoid. The following are equivalent.*

1. P is Markovian to \mathcal{G} .
2. For non-adjacent nodes i and j in \mathcal{G} such that $i \not\sim_p j$, it holds that $i \perp\!\!\!\perp j \mid \text{ant}(i, j)$.

Proof By Proposition 6, we have

$$\begin{aligned} i \text{ not adjacent to } j \text{ in } \text{max}(\mathcal{G}) &\iff i \text{ not adjacent to } j \text{ and } i \not\sim_p j \text{ in } \mathcal{G}, \text{ and} \\ i \perp\!\!\!\perp j \mid \text{ant}(i, j) \text{ (anterior of } \text{max}(\mathcal{G})) &\iff i \perp\!\!\!\perp j \mid \text{ant}(i, j) \text{ (anterior of } \mathcal{G}). \end{aligned} \quad (12)$$

Thus, by replacing both sides of the implication in (11) with the correspondence in (12), P satisfying the pairwise Markov property w.r.t. $\text{max}(\mathcal{G})$ is equivalent to Item 2.

By Proposition 7 and since \mathcal{G} and $\text{max}(\mathcal{G})$ are Markov equivalent, we have

$$\begin{aligned} P \text{ satisfies the pairwise Markov property w.r.t. } \text{max}(\mathcal{G}) &\iff P \text{ is Markovian to } \text{max}(\mathcal{G}) \\ &\iff P \text{ is Markovian to } \mathcal{G} \text{ (Item 1)}. \quad \square \end{aligned}$$

We will also use Sadeghi and Soo (2022, Theorem 27).

Proposition 9 ((Sadeghi and Soo, 2022)) *Let \mathcal{G} be an ancestral graph over the nodes V and P be a joint distribution over V induced from an SCM that corresponds to \mathcal{G} . The distribution P is Markovian to \mathcal{G} .*

Remark 13 *The proof of Proposition 9 uses Markov property results for acyclic directed mixed graphs from Richardson (2003) which do not depend on the maximality of graph \mathcal{G} .* \diamond

We first show that $J^\tau(\cdot | x_{\text{pa}(\tau)})$, the law of $f_\tau(x_{\text{pa}(\tau)}, \epsilon_\tau)$ of the structural equilibrium model, satisfies Lemma 10.

Lemma 10 Let \mathcal{G} be the corresponding graph (constructed using Algorithm 1) of a structural equilibrium model. Consider the chain component τ and associated distribution $J^\tau(\cdot | x_{\text{pa}(\tau)})$. For every node i , the conditional marginal $J_i^\tau(\cdot | x_{\tau \setminus i}; x_{\text{pa}(\tau)})$ does not depend on x_j for $j \in (\tau \cup \text{pa}(\tau)) \setminus (\text{pa}(i) \cup \text{ne}(i) \cup i)$.

Proof Consider a node $j \in \tau \setminus (\text{ne}(i) \cup i)$. By construction, in Step 1 of Algorithm 1, $J_i^\tau(\cdot | x_{\text{pa}(\tau)})$ satisfies $i \perp\!\!\!\perp j | \tau \setminus \{i, j\}$, which implies that $J_i^\tau(\cdot | x_{\tau \setminus i}; x_{\text{pa}(\tau)})$ does not depend on x_j .

Consider a node $j \in \text{pa}(\tau) \setminus \text{pa}(i)$. By Step 2 of Algorithm 1, the distribution $J_i^\tau(\cdot | x_{\tau \setminus i}; x_{\text{pa}(\tau)})$ does not depend on x_j . \square

For each node i , the conditional marginal $J_i^\tau(\cdot | x_{\tau \setminus i}; x_{\text{pa}(\tau)})$ depends only on the adjacent nodes in $\text{pa}(i) \cup \text{ne}(i)$.

Let $\text{sant}(i) = \text{ant}(i) \setminus \tau(i)$ be the strict anterior of the node i and let $\text{sant}(i, j) = \text{ant}(i, j) \setminus (\tau(i) \cup \tau(j))$.

Proof of Theorem 1 Let \mathcal{G} be a chain-connected antierial graph, and i and j be non-adjacent nodes such that $i \not\sim_p j$. By Proposition 8, it suffices to show that the distribution P induced from the structural equilibrium model satisfies $i \perp\!\!\!\perp j | \text{ant}(i, j)$.

We will consider the following cases.

1. Suppose that $j \in \text{ant}(i)$. We first consider $P_{\tau(i)}(\cdot | x_{\text{sant}(i)})$. Since $\text{ant}(i) \setminus \text{sant}(i) = \tau(i) \setminus i$, we then further condition $P_{\tau(i)}(\cdot | x_{\text{sant}(i)})$ given $x_{\tau(i) \setminus i}$ to obtain $P_i(\cdot | x_{\text{ant}(i, j) \cup j}) = P_i(\cdot | x_{\text{ant}(i)})$, since $j \in \text{ant}(i)$, and show that $P_i(\cdot | x_{\text{ant}(i)})$ does not depend on x_j .

Since there do not exist bidirected edges between nodes in $\text{sant}(i)$ and nodes in $\tau(i)$ by the antierial assumption, we have $\epsilon_{\tau(i)} \perp\!\!\!\perp X_{\text{sant}(i)}$. By definition, we have $X_{\tau(i)} = f_{\tau(i)}(X_{\text{pa}(\tau(i))}, \epsilon_{\tau(i)})$, and since the distribution of $\epsilon_{\tau(i)}$ remains the same after conditioning given $x_{\text{sant}(i)}$, we have

$$f_{\tau(i)}(x_{\text{pa}(\tau(i))}, \epsilon_{\tau(i)}) \sim P_{\tau(i)}(\cdot | x_{\text{sant}(i)}) = J^{\tau(i)}(\cdot | x_{\text{pa}(\tau(i))}). \quad (13)$$

Further conditioning on $x_{\tau(i) \setminus i}$, we obtain

$$P_i(\cdot | x_{\text{ant}(i)}) = J_i^{\tau(i)}(\cdot | x_{\text{pa}(\tau(i)) \cup \tau(i) \setminus i}). \quad (14)$$

Since i and j are not adjacent, $j \notin \text{ne}(i) \cup \text{pa}(i)$. By (14) and Lemma 10, $P_i(\cdot | x_{\text{ant}(i)})$ does not depend on x_j .

2. Suppose that $j \notin \text{ant}(i)$. If $i \in \text{ant}(j)$, then our previous argument (1) applies. Thus we also assume that $i \notin \text{ant}(j)$.

For the chain-connected antierial graph \mathcal{G} , consider the collapsed graph \mathcal{G}_{col} with nodes representing chain components; if $i \rightarrow j$ or $i \leftrightarrow j$ in \mathcal{G} , then we set $\tau(i) \rightarrow \tau(j)$ or $\tau(i) \leftrightarrow \tau(j)$ in \mathcal{G}_{col} , respectively. See Figure 14 for an example.

We make the following observations about \mathcal{G}_{col} .

- a. The graph \mathcal{G}_{col} does not have undirected edges and is an ancestral graph. This is because semi-directed paths from k and ℓ and bidirected edges $k \leftrightarrow \ell$ in \mathcal{G} correspond to directed paths from $\tau(k)$ to $\tau(\ell)$ and bidirected edges $\tau(k) \leftrightarrow \tau(\ell)$ (since \mathcal{G} is chain-connected) in \mathcal{G}_{col} respectively.
- b. For primitive inducing paths, we also have $i \not\sim_p j$ in \mathcal{G} implies that $\tau(i) \not\sim_p \tau(j)$ in \mathcal{G}_{col} ; to see this, we will show the contrapositive.

Let $\langle \tau(i), \tau(q_1), \dots, \tau(q_n), \tau(j) \rangle$ be a primitive inducing path in \mathcal{G}_{col} . We must have $\tau(i) \leftrightarrow \tau(q_1)$ and $\tau(j) \leftrightarrow \tau(q_n)$, since if $\tau(i) \rightarrow \tau(q_1)$ in \mathcal{G}_{col} , then in order for \mathcal{G}_{col} to not have directed cycles, $\tau(q_1)$ must be in $\text{ant}(\tau(j))$ in \mathcal{G}_{col} , which implies $i \in \text{ant}(j)$ in \mathcal{G} , a contradiction. The argument for

We can decompose the functional assignment $X_\tau = f_\tau^{\text{do}(C)}(X_{\text{pa}(\tau)}, \epsilon_\tau)$ in (8) separately into the parts $\tau \cap C$ and $\tau \setminus C$ as

$$\begin{aligned} X_{\tau \cap C} &= a_{\tau \cap C} \text{ and} \\ X_{\tau \setminus C} &= f_{\tau \setminus C}^{\text{do}(C)}(X_{\text{pa}(\tau)}, X_{\tau \cap C}, \epsilon_\tau), \end{aligned} \quad (15)$$

where $f_{\tau \setminus C}^{\text{do}(C)}(x_{\text{pa}(\tau)}, x_{\tau \cap C}, \epsilon_\tau) \sim J_{\tau \setminus C}^\tau(\cdot | a_{\tau \cap C}; x_{\text{pa}(\tau)})$ with the same error ϵ_τ . We will use the expression (15) to construct the corresponding graph \mathcal{G}_{do} and show Proposition 11.

Given a node i , let $\text{pa}_{\text{do}}(i)$ and $\text{ne}_{\text{do}}(i)$ denote the parents or neighbours of i in \mathcal{G}_{do} .

Proposition 11 *The corresponding graph \mathcal{G}_{do} of the intervened structural equilibrium model (8) is $\text{do}_C(\mathcal{G})$.*

Proof Since the graphs \mathcal{G}_{do} and $\text{do}_C(\mathcal{G})$ have the same nodes, it suffices to show that both graphs have the same set of undirected, directed, and bidirected edges.

To show that the sets of undirected and directed edges coincide, given a node $i \in \tau$ for some chain component τ in \mathcal{G} , we show how $\text{pa}_{\text{do}}(i)$ and $\text{ne}_{\text{do}}(i)$ is related to $\text{pa}(i)$ and $\text{ne}(i)$, the parents and neighbours of i in \mathcal{G} , as follows.

- If $i \notin C$, then $\text{ne}_{\text{do}}(i) = \text{ne}(i) \setminus C$. If $i \in C$, then $\text{ne}_{\text{do}}(i) = \emptyset$.

For nodes $i \in \tau \setminus C$, Step 1 of Algorithm 1 uses $J_{\tau \setminus C}^\tau(\cdot | a_{\tau \cap C}; x_{\text{pa}(\tau)})$ to construct $\text{ne}_{\text{do}}(i)$ as the set of nodes $j \in \tau \setminus C$ satisfying

$$i \perp\!\!\!\perp j | (\tau \setminus C) \setminus \{i, j\} \text{ for the conditional distribution } J_{\tau \setminus C}^\tau(\cdot | a_{\tau \cap C}; x_{\text{pa}(\tau)}).$$

This is equivalent to j satisfying $i \perp\!\!\!\perp j | \tau \setminus \{i, j\}$ for $J^\tau(\cdot | x_{\text{pa}(\tau)})$, which is how Algorithm 1 determines whether $j \in \tau \setminus C$ should be in $\text{ne}(i)$ when using $J^\tau(\cdot | x_{\text{pa}(\tau)})$. Thus $\text{ne}_{\text{do}}(i) = \text{ne}(i) \cap (\tau \setminus C) = \text{ne}(i) \setminus C$.

For $i \in C$, applying Step 1 of Algorithm 1 to the law $\delta_i(a_i)$ of the functional assignment $X_{\tau \cap C} = a_{\tau \cap C}$ results in $\text{ne}_{\text{do}}(i) = \emptyset$.

- If $i \notin C$, then $\text{pa}_{\text{do}}(i) = \text{pa}(i) \cup (\text{ne}(i) \cap C)$. If $i \in C$, then $\text{pa}_{\text{do}}(i) = \emptyset$.

For nodes $i \in \tau \setminus C$, Step 2 of Algorithm 1 uses $J_{\tau \setminus C}^\tau(\cdot | a_{\tau \cap C}; x_{\text{pa}(\tau)})$ to select $\text{pa}_{\text{do}}(i)$ as the set of nodes $j \in \text{pa}(\tau) \cup (\tau \cap C)$ such that for every value $x_{(\tau \cup \text{pa}(\tau)) \setminus \{i, j\}}$, we have

$$J_i^\tau(\cdot | x_{(\tau \setminus C) \setminus i}, a_{\tau \cap C}; x_{\text{pa}(\tau)}) = J_i^\tau(\cdot | x_{\tau \setminus i}; x_{\text{pa}(\tau)})$$

depends on the value of x_j . This is how Algorithm 1 determines whether $j \in \text{pa}(\tau)$ should be in $\text{pa}(i)$. For nodes $j \in \tau \cap C$, from Lemma 10, it can be seen that $J_i^\tau(\cdot | x_{\tau \setminus i}; x_{\text{pa}(\tau)})$ depends only on nodes $j \in \text{ne}(i)$. Thus $\text{pa}_{\text{do}}(i) = \text{pa}(i) \cup (\text{ne}(i) \cap C)$.

For $i \in C$, applying Step 2 of Algorithm 1 to the law $\delta_i(a_i)$ of the functional assignment $X_{\tau \cap C} = a_{\tau \cap C}$ results in $\text{pa}_{\text{do}}(i) = \emptyset$.

Observe that this relationship is also exactly described by Algorithm 2. For example, from Figure 7, it can be seen that $\text{ne}_{\text{do}}(5) = \{3\} \setminus 3 = \text{ne}(5) \setminus C$ and $\text{pa}_{\text{do}}(5) = \emptyset \cup 2 = \text{pa}(5) \cup (\text{ne}(5) \cap C)$.

We next show that the bidirected edges coincide. For each part τ of \mathcal{G} , the errors ϵ_τ for the functional assignment of $X_{\tau \setminus C}$ in (15) have the same joint distribution, and thus dependencies, as the errors in the observational structural equilibrium model. Thus applying Step 3 of Algorithm 1 to the errors ϵ_τ of (15) returns the same bidirected edges as \mathcal{G} only with the bidirected edges connected to the nodes in $\tau \cap C$ removed (since the functional assignment of $X_{\tau \cap C}$ in (15) is deterministic). These remaining edges coincide with the bidirected edges of $\text{do}_C(\mathcal{G})$. \square

Lemma 12 Let \mathcal{G} be a chain-connected arterial graph. Then $\text{do}_C(\mathcal{G})$ is a chain-connected arterial graph.

Proof We make the following observations.

1. Edges with endpoint nodes not in C are the same in both \mathcal{G} and $\text{do}_C(\mathcal{G})$.
2. Semi-directed paths and cycles (if they exist) in $\text{do}_C(\mathcal{G})$ cannot contain nodes in C .
3. Nodes i in C are only connected to directed edges pointing away from i .

Recall Definition 1; we first verify that the graph is arterial. Observations 1 and 2 imply that $\text{do}_C(\mathcal{G})$ does not contain any semi-directed cycle in \mathcal{G} . Towards a contradiction, suppose that there exists a bidirected edge $j \leftrightarrow k$ with semi-directed path between j and k in $\text{do}_C(\mathcal{G})$, then Observation 3 implies that $j, k \notin C$, from which, using Observation 1, we have that bidirected edge $j \leftrightarrow k$ is in \mathcal{G} . Observations 1 and 2 imply the same semi-directed path between endpoints of $j \leftrightarrow k$ in \mathcal{G} , which is absurd, since \mathcal{G} is arterial.

Recall Definition 8; we finally verify that the graph is chain-connected. Towards a contradiction, suppose that there exists node configuration $i \leftrightarrow j - k$ in $\text{do}_C(\mathcal{G})$. From observation 3, i, j and k cannot be in C , thus observation 1 implies that the node configuration $i \leftrightarrow j - k$ exists in \mathcal{G} , which implies that $i \leftrightarrow k$ in \mathcal{G} and thus by observation 1 in $\text{do}_C(\mathcal{G})$ as well. \square

Proof of Theorem 2 By Proposition 11, we have that $\text{do}_C(\mathcal{G})$ is the corresponding graph of the intervened structural equilibrium model (8). By Lemma 12, we have that $\text{do}_C(\mathcal{G})$ is a chain-connected arterial graph. Thus an application of Theorem 1 completes the proof. \square

A.3. Proof of Theorem 3

Consider an observational structural equilibrium model with the corresponding graph \mathcal{G} . Similar to the proof of Theorem 2, we first show that after applying Algorithm 1 to the combined structural equilibrium model (9), the returned corresponding graph \mathcal{G}_ϕ is, in fact, the graph $\phi(\mathcal{G}; C)$ obtained from Algorithm 2.

Proposition 13 *The corresponding graph \mathcal{G}_ϕ of the combined structural equilibrium model (9) is $\phi(\mathcal{G}; C)$.*

Proof Given an observational structural equilibrium model with the corresponding graph \mathcal{G} , consider the combined structural equilibrium model in (9).

We first show that the nodes coincide. Consider the set of nodes $i \notin C$ such that $C \cap \text{ant}(i) = \emptyset$ in \mathcal{G} , call this set A , which is the set in Step 2 of Algorithm 3. For $i \in A$, it holds that $X_{\tau(i)} = X_{\tau(i)}^{\text{do}(C)}$ and the arguments (in A) of the functional assignments of $X_{\tau}^{\text{do}(C)}$ in (9) can be substituted as

$$\begin{aligned} X_{\tau}^{\text{do}(C)} &= f_{\tau}^{\text{do}(C)}(X_{\text{pa}(\tau) \setminus A}^{\text{do}(C)}, X_{\text{pa}(\tau) \cap A}, \epsilon_{\tau}), \quad \text{if } \tau \cap C \neq \emptyset \text{ and} \\ X_{\tau}^{\text{do}(C)} &= f_{\tau}(X_{\text{pa}(\tau) \setminus A}^{\text{do}(C)}, X_{\text{pa}(\tau) \cap A}, \epsilon_{\tau}), \quad \text{if } \tau \cap C = \emptyset. \end{aligned} \tag{16}$$

Thus, (9) has exactly the same variables as the nodes in $\phi(\mathcal{G}; C)$.

We show that the undirected and directed edges coincide. From (16), since the law of the functional assignments remains the same as the intervened structural equilibrium model (8), applying Steps 1 and 2 of Algorithm 1 to the combined structural equilibrium model results in, for nodes $i^{\text{do}(C)}$, the same $\text{ne}_{\text{do}}(i^{\text{do}(C)})$ and $\text{pa}_{\text{do}}(i^{\text{do}(C)})$ as the relabelled $\text{do}_C(\mathcal{G})$ (by similar argument of Proposition 11), except with nodes $j^{\text{do}(C)} \in \text{pa}_{\text{do}}(i^{\text{do}(C)})$, where $j \in A$, being replaced with j . Thus, applying Steps 1 and 2 of Algorithm 1 to (9) results in the same undirected and directed edges as after applying Steps 1 and 2 of Algorithm 3.

We next show that the bidirected edges coincide. The dependence of the errors between two observational variables and two intervened variables is the same as the observational structural equilibrium model and the intervened structural equilibrium model (8) respectively, thus when applying Algorithm 1, the added bidirected edges coincide with those of \mathcal{G} and $\text{do}_C(\mathcal{G})$ respectively. The error ϵ_{τ} for X_{τ} and $X_{\tau}^{\text{do}(C)}$ is shared in (9). The resulting dependence of errors between observational and intervened variables, when used to create bidirected edges using Algorithm 1, is accounted for in Table 1 of Step 3 of Algorithm 3. \square

Proposition 14 (The single world graph $\phi(\mathcal{G}; C)$ is a chain-connected antierial graph) *If \mathcal{G} is a chain-connected antierial graph, then for any node subset $C \subseteq V$, we have that $\phi(\mathcal{G}; C)$ is a chain-connected antierial graph.*

Proof of Proposition 14 Note that nodes in $\phi(\mathcal{G}; C)$ are either nodes from \mathcal{G} or from $\text{do}_C(\mathcal{G})$, which we will differentiate with a superscript $\cdot^{\text{do}(C)}$ (with $i^{\text{do}(C)}$ being a node from $\text{do}_C(\mathcal{G})$ that corresponds with the node i from \mathcal{G}).

We have the following observations.

1. By Lemma 12, both \mathcal{G} and $\text{do}_C(\mathcal{G})$ are chain-connected antierial graphs.
2. For nodes $i, j \notin C$, an edge between i and j in \mathcal{G} correspond to the same edge between $i^{\text{do}(C)}$ and $j^{\text{do}(C)}$ in $\text{do}_C(\mathcal{G})$.
3. From Step 2, edges between nodes i and $j^{\text{do}(C)}$ in $\phi(\mathcal{G}; C)$ are either $i \rightarrow j^{\text{do}(C)}$ or $i \leftrightarrow j^{\text{do}(C)}$. See, for example, the middle of Figure 8. This is because $i, j \notin C$ and $j \notin \text{ant}(i)$, otherwise $j \in \text{ant}(i)$ and $C \cap \text{ant}(j) \neq \emptyset$ (by the condition in Step 2) causing $C \cap \text{ant}(i) \neq \emptyset$, contradicting the condition in Step 2.
4. An edge between nodes i and j in $\phi(\mathcal{G}; C)$ corresponds to the same edge in \mathcal{G} . If $i^{\text{do}(C)}$ and $j^{\text{do}(C)}$ are nodes in $\phi(\mathcal{G}; C)$, then this correspondence of edges between $\phi(\mathcal{G}; C)$ and $\text{do}_C(\mathcal{G})$ also holds.

We will show that there are no semi-directed cycles in $\phi(\mathcal{G}; C)$. By Observations (1) and (4), we only have to show semi-directed cycles consisting of both nodes of the form i and $j^{\text{do}(C)}$ do not exist in $\phi(\mathcal{G}; C)$. This is implied by (3).

We will show that there are no semi-directed paths connecting endpoints of a bidirected edge in $\phi(\mathcal{G}; C)$. Consider edges of the form $i \leftrightarrow j$ or $i^{\text{do}(C)} \leftrightarrow j^{\text{do}(C)}$ in $\phi(\mathcal{G}; C)$. By (3), a semi-directed path between i and j or $i^{\text{do}(C)}$ and $j^{\text{do}(C)}$ in $\phi(\mathcal{G}; C)$ must only consists of nodes of the form k or $k^{\text{do}(C)}$ respectively. By (4), such a semi-directed path connects the endpoints of $i \leftrightarrow j$ or $i^{\text{do}(C)} \leftrightarrow j^{\text{do}(C)}$ in \mathcal{G} or $\text{do}_C(\mathcal{G})$, respectively, and thus cannot exist by (1). For the edge $i \leftrightarrow j^{\text{do}(C)}$, by (3), a semi-directed path from i to $j^{\text{do}(C)}$ cannot contain nodes of the form $k^{\text{do}(C)}$ where $k \in C$ (since there are no undirected or directed edges pointing into $k^{\text{do}(C)}$ in $\text{do}_C(\mathcal{G})$ and by (4) in $\phi(\mathcal{G}; C)$ as well), thus by (2) would imply a semi-directed path from endpoints of $i \leftrightarrow j$ in \mathcal{G} .

Chain-connectedness of $\phi(\mathcal{G}; C)$ follows trivially from item 3 of Table 1, along with \mathcal{G} and $\text{do}_C(\mathcal{G})$ being chain-connected by (1). \square

We will show Theorem 3 using Theorem 1 and Proposition 11.

Proof of Theorem 3 By Proposition 13, we have that $\phi(\mathcal{G}; C)$ is the corresponding graph of the intervened structural equilibrium model (9). By Proposition 14, we have that $\phi(\mathcal{G}; C)$ is a chain-connected antierial graph. An application of Theorem 1 completes the proof. \square

Proof of Proposition 4 By Theorem 3, since P^* is Markovian to $\phi(\mathcal{G}; C)$, the marginal P_{sub}^* is Markovian to $\phi'(G; C) = \alpha_m(\phi(\mathcal{G}; C); \text{po}(C))$. \square

A.4. Proof of Theorem 5

To prove Theorem 5, we will use the following results from Sadeghi (2016, Theorem 1) which shows how α_m composes, as a function, with itself.

Proposition 15 ((Sadeghi, 2016)) *Consider the graph \mathcal{G} over the nodes V . Given disjoint subsets $M_1, M_2 \subseteq V$, we have that $\alpha_m(\alpha_m(\mathcal{G}; M_1); M_2) = \alpha_m(\mathcal{G}; M_1 \cup M_2)$.*

Lemma 16 Consider the graph \mathcal{G} over V and subsets $L, U \subseteq V$ such that $L \subseteq U$. The node i not being adjacent to the node j in $\max(\alpha_m(\alpha_c(\mathcal{G}; L); V \setminus U))$ is equivalent to the existence of a set $S \subseteq V$ such that $i \perp_{\mathcal{G}} j \mid S$ and $L \subseteq S \subseteq U$.

Proof We have the following equivalence. Let \mathcal{G}_0 denote the graph $\alpha_m(\alpha_c(\mathcal{G}; L); V \setminus U)$.

$$\begin{aligned}
i \text{ and } j \text{ not adjacent in } \max(\mathcal{G}_0) &\iff i \perp_{\max(\mathcal{G}_0)} j \mid A \text{ for some } A \subseteq U \setminus L \\
&\iff i \perp_{\alpha_m(\alpha_c(\mathcal{G}; L); V \setminus U)} j \mid A \\
&\iff i \perp_{\alpha_c(\mathcal{G}; L)} j \mid A \\
&\iff i \perp_{\mathcal{G}} j \mid A \cup L,
\end{aligned}$$

where the first equivalence follows by Definition 2 of maximal graphs, the second equivalence follows by Markov equivalence of $\max(\mathcal{G}')$ and \mathcal{G}' for any graph \mathcal{G}' and the last two equivalences follow by the definitions of operations α_m in (1) (since $i, j, A \subseteq (V \setminus L) \setminus (V \setminus U)$) and α_c in (2) (since $i, j, A \subseteq V \setminus L$). Taking $S = A \cup L$, we have $i \perp_{\mathcal{G}} j \mid S$ and $L \subseteq S \subseteq U$. \square

Proof of Theorem 5 Let the joint distribution of $X_O^{\text{do}(C)}, X_C, X_U$ and potentially other variables be Markovian to some ancestral graph \mathcal{G}^* (over nodes V^*) and denote the nodes representing $X_O^{\text{do}(C)}$ and X_C as $O^{\text{do}(C)}$ and C respectively. To select an adjustment set S , it suffices to select a set S such that $O^{\text{do}(C)} \perp_{\mathcal{G}^*} C \mid S$.

Consider the graph $\mathcal{G}_0^* = \alpha_m(\alpha_c(\mathcal{G}^*; L); V^* \setminus (U \cup C \cup O^{\text{do}(C)}))$ in Algorithm 4. Lemma 16 guarantees that non-adjacency of $O^{\text{do}(C)}$ and C in $\max(\mathcal{G}_0^*)$ guarantees the existence of an adjustment set S such that $L \subseteq S \subseteq U$.

Let S_n denote the candidate output set S at step n of Algorithm 4. Given the node $i_n \in S_n \setminus L$ at step n , if $O^{\text{do}(C)}$ is not adjacent to C in $\max(\alpha_m(\mathcal{G}_n^*; i_n))$, then by Proposition 15, we have $\alpha_m(\mathcal{G}_n^*; i_n) = \alpha_m(\alpha_c(\mathcal{G}^*; L); (V^* \setminus (S_n \cup C \cup O^{\text{do}(C)})) \cup i_n)$. Applying Lemma 16, there exists a set S such that $O^{\text{do}(C)} \perp_{\mathcal{G}^*} C \mid S$ and $L \subseteq S \subseteq S_n \setminus i_n \subset U$. Thus, at step n when some node i_n can be excluded from S_n , Algorithm 4 guarantees the existence of an adjustment set S that satisfies $L \subseteq S \subseteq U$ and decreases the cardinality of S_n by one. Consider the first step n such that there are no nodes that can be excluded from S_n , then by Proposition 15 and Lemma 16, it holds that $O^{\text{do}(C)} \not\perp_{\mathcal{G}^*} C \mid S$ for every set S such that $L \subseteq S \subseteq S_n \setminus i_n$ for any node $i_n \in S_n$. However, the existence of a set $S \subseteq S_n$ satisfying $O^{\text{do}(C)} \perp_{\mathcal{G}^*} C \mid S$ is ensured in step $n - 1$, thus S_n must be an adjustment set.

Let the joint distribution of $X_O^{\text{do}(C)}, X_C, X_U$ and potentially other variables be faithful to the ancestral graph \mathcal{G}^* . Consider again the first step n such that no nodes can be excluded from S_n , then $O^{\text{do}(C)} \not\perp_{\mathcal{G}^*} C \mid S$ for every set S such that $L \subseteq S \subseteq S_n \setminus i_n$ for any node $i_n \in S_n$. By faithfulness, every set S such that $L \subseteq S \subset S_n$ is not an adjustment set. However the existence of an adjustment set $S \subseteq S_n$ is guaranteed from step $n - 1$, thus S_n must be a minimal adjustment set.

If $O^{\text{do}(C)}$ is adjacent to C in $\max(\mathcal{G}_0^*)$, then by Lemma 16, we have $O^{\text{do}(C)} \not\perp_{\mathcal{G}^*} C \mid S$ and by faithfulness, $O^{\text{do}(C)} \not\perp C \mid S$, for every set S such that $L \subseteq S \subseteq U$, thus an adjustment set S satisfying $L \subseteq S \subseteq U$ does not exist. \square

A.5. The ancestral assumption and causal interpretability

In general, the corresponding graph of a structural equilibrium model is a chain mixed graph (see Definition 9), to which the induced joint distribution P may not be Markovian. We can generalise Algorithm 1 to Algorithm 5, which, in general, returns a Markovian chain mixed graph that P is Markovian to.

When the corresponding graph is ancestral, by equality (13) in the proof of Theorem 1, the following equality holds for part τ of the structural equilibrium model,

$$P_\tau(\cdot \mid x_{\text{ant}(\tau)}) = J^\tau(\cdot \mid x_{\text{pa}(\tau)}),$$

which also implies that $i \perp\!\!\!\perp j \mid \text{ant}(i, j)$ holds for nodes i and j in Step 4 of Algorithm 5. Thus, when the corresponding graph is ancestral, Algorithm 5 reduces to Algorithm 1.

Remark 15 The additional Step 4 in Algorithm 5 allows the argument in the proof of Theorem 1 using \mathcal{G}_{col} to be applied to the case when $i \in \text{ant}(j)$. The rest of the proof of Theorem 1 follows. \diamond

Algorithm 5 Modification of Algorithm 1 for chain mixed graphs**Input:** Structural equilibrium model inducing a joint distribution P .**Output:** Chain-connected chain mixed graph \mathcal{G} .

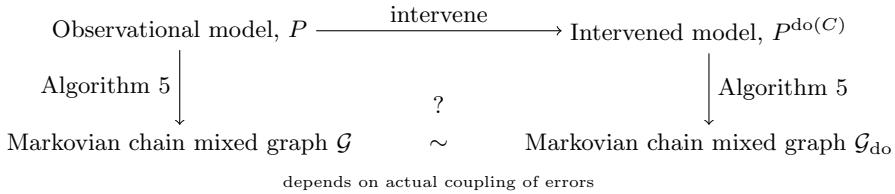
- 1: Perform Step 1 of Algorithm 1 with $P_\tau(\cdot | x_{\text{ant}(\tau)})$ in place of $J^\tau(\cdot | x_{\text{pa}(\tau)})$.
- 2: Perform Step 2 of Algorithm 1 with $P_i(\cdot | x_{(\tau \setminus i) \cup \text{ant}(\tau)})$ in place of $J_i^\tau(\cdot | x_{\tau \setminus i}; x_{\text{pa}(\tau)})$.
- 3: Perform Step 3 of Algorithm 1.
- 4: Call the resulting graph \mathcal{G}' . In \mathcal{G}' , for nodes i and j such that

1. $i \in \text{ant}(j) \setminus \text{pa}(j)$, and
2. there exists a primitive inducing path $\pi = \langle i', q_1, \dots, q_n, j \rangle$ between nodes $i' \in \tau(i)$ and j such that $i' \rightarrow q_1$.

if $i \not\perp\!\!\!\perp j | \text{ant}(i, j)$ holds for P , then create the edge $i \rightarrow q_1$.

The additional edges created in Step 4 of Algorithm 5 depend on the joint distribution P which depends on the actual coupling, and not just the dependencies of the error variables. Thus, the edges in Step 4 of Algorithm 5 lack mechanistic causal interpretability.

Proposition 11 implies that Algorithm 2 obtains the corresponding graph \mathcal{G}_{do} of the intervened structural equilibrium model from the observational graph \mathcal{G} , *without* referring to the interventional distribution $P^{\text{do}(C)}$. This is possible since in the case of arterial graphs, Algorithm 1 constructs the corresponding \mathcal{G}_{do} by only referring to the law of functional assignments $J^{\tau, \text{do}(C)}(\cdot | x_{\text{pa}(\tau)})$, which behaves as described in (7), as accounted for by Algorithm 2 in a local and mechanistic manner. However, in the case of chain mixed graphs, Algorithm 5 constructs \mathcal{G}_{do} *with* reference to the interventional distribution $P^{\text{do}(C)}$. It is unclear how to graphically relate \mathcal{G} and \mathcal{G}_{do} , since we would have to account for how conditional independencies in $P^{\text{do}(C)}$ relate to conditional independencies in P , and this relationship depends on the actual coupling, and not just dependencies of the error variables as in the case of arterial graphs. Contrast the illustration below with Figure 15.

**A.6. Including all nodes in SWIG using parallel-worlds graphs**

Consider the case of DAGs. Modifying the parallel-worlds graph approach (Avin et al., 2005), we present an extension of the construction in Algorithm 3 that includes all the nodes in SWIGs, complementing the comparison between SWIGs and counterfactual graphs in Richardson and Robins (2013).

Given a DAG \mathcal{G} , it is possible to order all the nodes j and k in the treatment set C such that $k > j$ if there does not exist a directed path from j to k in \mathcal{G} . With respect to such an ordering of $C = \{x_1, \dots, x_n\}$, we can construct all the parallel-worlds graphs $\mathcal{G}, \text{do}_{[1]}(\mathcal{G}), \dots, \text{do}_{[n]}(\mathcal{G})$, where $\text{do}_{[i]}(\mathcal{G}) = \text{do}_{\{x_1, \dots, x_i\}}(\mathcal{G})$ and by convention $\text{do}_{[0]}(\mathcal{G}) = \mathcal{G}$. In each graph $\text{do}_{[i]}(\mathcal{G})$, nodes that correspond to node j in \mathcal{G} are relabelled as $j^{[i]}$ (with $j^{[0]} = j$).

The nodes in the parallel-worlds graphs are then merged and removed as follows:

1. Consider de_i , the set of descendants of $x_i^{[i]}$, including $x_i^{[i]}$, that are not descendants of $\{x_{i+1}^{[i]}, \dots, x_n^{[i]}\}$ in $\text{do}_{[i]}(\mathcal{G})$. Let de_0 be the set of nodes that are not descendants of $\{x_1, \dots, x_n\}$ in \mathcal{G} .
2. Repeatedly merge, for each $i \in \{0, \dots, n-1\}$, as follows. Consider the node $j^{[i]} \in \text{de}_i$.
 - If $j \notin C$, then merge nodes $j^{[k]}$ of graphs $\text{do}_{[k]}(\mathcal{G})$ for all $k \in \{i+1, \dots, n\}$ into node $j^{[i]}$ as in Step 2 of Algorithm 3.

- If $j = x_\ell \in C$, then merge nodes $x_\ell^{[k]}$ of graphs $\text{do}_{[k]}(\mathcal{G})$ for all $k \in \{i+1, \dots, \ell-1\}$ into node $j^{[i]}$ as in Step 2 of Algorithm 3.

3. Take the subgraph of the nodes in $\bigcup_{i=0}^{n-1} \text{de}_i$ and the remaining nodes in $\text{do}_{[n]}(\mathcal{G})$.

Call the resulting subgraph $\mathcal{G}(C)$. See Figure 16 for an illustration for this extension of Algorithm 3 in the case of DAGs.

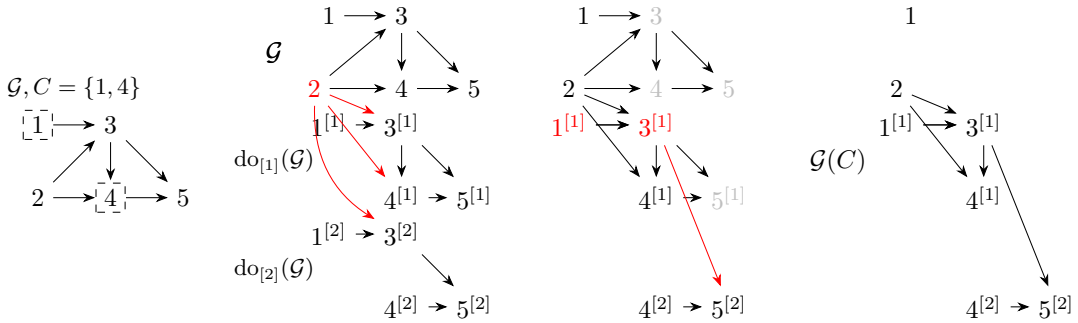


Fig. 16: Left: DAG \mathcal{G} with $C = \{1, 4\}$. Middle 2 graphs: Sequentially merging nodes from different graphs, as in step 2 of Algorithm 3. With $\text{de}_0 = \{1, 2\}$ and $\text{de}_1 = \{1^{[1]}, 3^{[1]}, 4^{[1]}\}$, the nodes $2^{[1]}, 2^{[2]}$ are merged into 2 and the nodes $1^{[2]}, 3^{[2]}$ are merged into $1^{[1]}, 3^{[1]}$ respectively. Right: Output $\mathcal{G}(C)$ after taking the subgraph over nodes in $\text{de}_0 \cup \text{de}_1$ and the remaining nodes in $\text{do}_{[2]}(\mathcal{G})$.

We then have the following relating this construction to single-world intervention graphs (Richardson and Robins, 2013).

Proposition 17 *Given a DAG \mathcal{G} and an ordered treatment set $C = \{x_1, \dots, x_n\}$, the output $\mathcal{G}(C)$ is the single-world intervention graph.*

Proof Observe that in a single-world intervention graph, after splitting the node x_i in C , nodes j that are descendants of x_i , including x_i , but are not descendants of $\{x_{i+1}, \dots, x_n\}$ are relabelled as $j^{[i]}$. These coincide with the nodes in de_i . While nodes that are not relabelled coincide with the nodes in de_0 from \mathcal{G} . Thus, since $\mathcal{G}(C)$ is a subgraph over $\bigcup_{i=0}^{n-1} \text{de}_i$ and the remaining nodes in $\text{do}_{[n]}(\mathcal{G})$, the graph $\mathcal{G}(C)$ contains exactly all the nodes in the single-world intervention graph.

In the single-world intervention graph, the parent $k^{[m]}$ (for $m \leq i$) of the node $j^{[i]}$ corresponds to the parents $k^{[i]}$ of node $j^{[i]}$ in $\text{do}_{[i]}(\mathcal{G})$. Since $k^{[i]}$ is merged with $k^{[m]}$ in $\mathcal{G}(C)$, the parental relationships in $\mathcal{G}(C)$ are the same with that in the single-world intervention graph. \square

Repeating the same argument for Proposition 4, we see that taking the subgraph over $\bigcup_{i=0}^{n-1} \text{de}_i$ and the remaining nodes in $\text{do}_{[n]}(\mathcal{G})$ amounts to marginalising the merged graph. Thus, Propopostion 17 formally relates counterfactual graphs (Shpitser and Pearl, 2007) and single-world intervention graphs (Richardson and Robins, 2013) by marginalisation.

A.7. Simulation Results

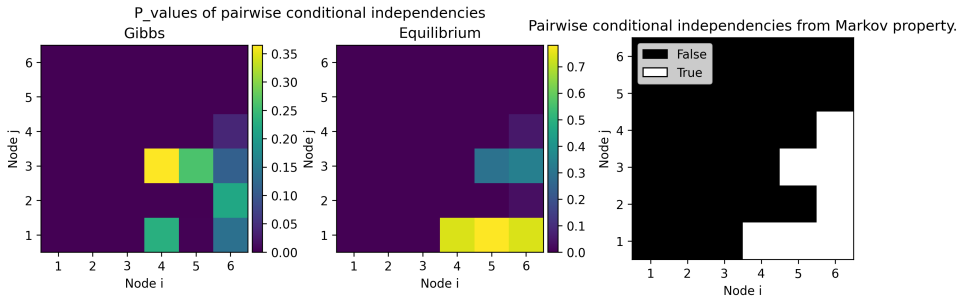


Fig. 17: P-values from hypothesis testing of pairwise conditional independencies of the form $i \perp\!\!\!\perp j \mid \text{ant}(i, j)$. The data is sampled from the structural equilibrium model in Figure 4 using, Left: Gibbs sampling. Middle: the equilibrium distributions $J^T(\cdot \mid x_{\text{pa}(\tau)})$. Right: Pairwise conditional independencies of the form $i \perp\!\!\!\perp j \mid \text{ant}(i, j)$ if Markov property w.r.t. the corresponding \mathcal{G}_1 holds.

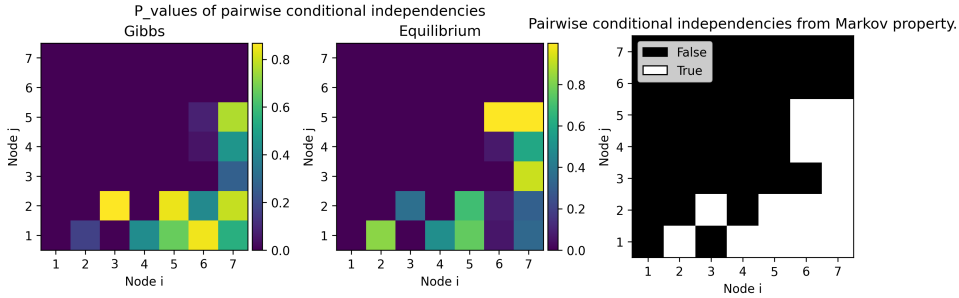


Fig. 18: P-values from hypothesis testing of pairwise conditional independencies of the form $i \perp\!\!\!\perp j \mid \text{ant}(i, j)$. The data is sampled from the structural equilibrium model in Figure 5 using, Left: Gibbs sampling. Middle: the equilibrium distributions $J^T(\cdot \mid x_{\text{pa}(\tau)})$. Right: Pairwise conditional independencies of the form $i \perp\!\!\!\perp j \mid \text{ant}(i, j)$ if Markov property w.r.t. the corresponding \mathcal{G}_2 holds.

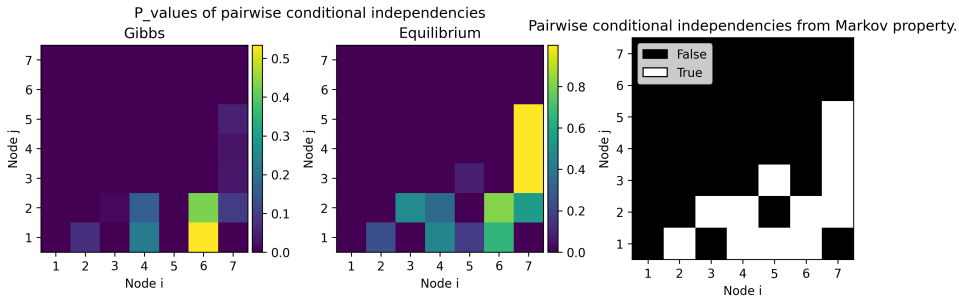


Fig. 19: P-values from hypothesis testing of pairwise conditional independencies of the form $i \perp\!\!\!\perp j \mid \text{ant}(i, j)$. The data is sampled from the structural equilibrium model in Figure 6 using, Left: Gibbs sampling. Middle: the equilibrium distributions $J^T(\cdot \mid x_{\text{pa}(\tau)})$. Right: Pairwise conditional independencies of the form $i \perp\!\!\!\perp j \mid \text{ant}(i, j)$ if Markov property w.r.t. the corresponding \mathcal{G}_3 holds.

References

- C. Avin, I. Shpitser, and J. Pearl. Identifiability of path-specific effects. In *International Joint Conference on Artificial Intelligence*, pages 357–363, 2005.
- A. Balke and J. Pearl. Probabilistic evaluation of counterfactual queries. In *Proceedings of the Twelfth AAAI National Conference on Artificial Intelligence*, pages 230–237. AAAI Press, 1994.
- P. Constantinou and A. P. Dawid. Extended conditional independence and applications in causal inference. *The Annals of Statistics*, 45(6):2618–2653, 2017.
- A. P. Dawid. Conditional independence in statistical theory. *Journal of the Royal Statistical Society. Series B (Methodological)*, 41(1):1–31, 1979.
- A. P. Dawid. Discussion on the paper by Lauritzen and Richardson. *Journal of the Royal Statistical Society Series B: (Statistical Methodology)*, 64(3):348–352, 2009.
- M. Frydenberg. The chain graph Markov property. *Scandinavian Journal of Statistics*, 17(4):333–353, 1990.
- S. Geman and D. Geman. Stochastic relaxation, Gibbs distributions, and the Bayesian restoration of images. *IEEE Transactions on Pattern Analysis and Machine Intelligence*, PAMI-6(6):721–741, 1984.
- F. R. Guo and Q. Zhao. Confounder selection via iterative graph expansion. *The Annals of Statistics*, 54(1):516–541, 2026.
- M. A. Hernan and J. M. Robins. *Causal Inference: What If*. Chapman & Hall/CRC, 2020.
- P. W. Holland. Statistics and causal inference. *Journal of the American Statistical Association*, 81(396):945–960, 1986.
- S. Lauritzen and K. Sadeghi. Unifying Markov properties for graphical models. *The Annals of Statistics*, 46(5):2251–2278, 2018.
- S. L. Lauritzen. *Graphical Models*. Oxford University Press, 1996. ISBN 0-19-852219-3.
- S. L. Lauritzen and T. S. Richardson. Chain graph models and their causal interpretations. *Journal of the Royal Statistical Society: Series B (Statistical Methodology)*, 64(3):321–348, 2002.
- G. M. Marchetti, M. Drton, and K. Sadeghi. Graphical markov models with mixed graphs. <https://cran.r-project.org/web/packages/ggm/index.html>, 2025.
- C. Meek and K. Sadeghi. Characterizing and identifying separable graphical models, 2026. URL <https://www.youtube.com/watch?v=96WrC5PTaec>.
- J. Pearl. *Causality*. Cambridge University Press, Cambridge, second edition, 2009. Models, reasoning, and inference.
- T. Richardson. Markov properties for acyclic directed mixed graphs. *Scandinavian Journal of Statistics*, 30(1):145–157, 2003.
- T. Richardson and P. Spirtes. Ancestral graph Markov models. *The Annals of Statistics*, 30(4):962–1030, 2002.
- T. S. Richardson and J. M. Robins. Single world intervention graphs (SWIGs): A unification of the counterfactual and graphical approaches to causality. *Center for the Statistics and the Social Sciences, University of Washington Series. Working Paper 128*, 2013.
- T. S. Richardson and J. M. Robins. Potential outcome and decision theoretic foundations for statistical causality. *Journal of Causal Inference*, 11(1):20220012, 2023.
- A. Rotnitzky and E. Smucler. Efficient adjustment sets for population average causal treatment effect estimation in graphical models. *Journal of Machine Learning Research*, 21(188):1–86, 2020.
- D. B. Rubin. Bayesian inference for causal effects: The role of randomization. *The Annals of Statistics*, 6(1):34–58, 1978.
- D. B. Rubin. Causal inference using potential outcomes. *Journal of the American Statistical Association*, 100(469):322–331, 2005.
- D. B. Rubin. Should observational studies be designed to allow lack of balance in covariate distributions across treatment groups? *Statistics in Medicine*, 28:1420–1423, 2009.
- K. Sadeghi. Marginalization and conditioning for LWF chain graphs. *The Annals of Statistics*, 44(4):1792–1816, 2016.
- K. Sadeghi. Faithfulness of probability distributions and graphs. *Journal of Machine Learning Research*, 18(148):1–29, 2017.
- K. Sadeghi and T. Soo. Conditions and assumptions for constraint-based causal structure learning. *Journal of Machine Learning Research*, 23(109):1–34, 2022.
- I. Shpitser. Segregated graphs and marginals of chain graph models. In *Proceedings of the 29th International Conference on Neural Information Processing Systems - Volume 1*, pages 1720–1728, Cambridge, MA, USA, 2015. MIT Press.
- I. Shpitser and J. Pearl. What counterfactuals can be tested. In *Proceedings of the Twenty-Third Conference on Uncertainty in Artificial Intelligence*, pages 352–359. AUAI Press, 2007.
- P. Spirtes, C. Glymour, and R. Scheines. *Causation, Prediction, and Search*. MIT Press, Cambridge, MA, second edition, 2000.

-
- K. Teh. constrained confounder selection. <https://github.com/KaiZTeh/CCS>, 2026.
- U.S. Food and Drug Administration. Adjusting for covariates in randomized clinical trials for drugs and biological products guidance for industry. Docket Number: FDA-2019-D-0934, 2023. URL <https://www.fda.gov/regulatory-information/search-fda-guidance-documents/adjusting-covariates-randomized-clinical-trials-drugs-and-biological-products>.
- B. van der Zander, M. Liškiewicz, and J. Textor. Separators and adjustment sets in causal graphs: Complete criteria and an algorithmic framework. *Artificial Intelligence*, 270:1–40, 2019.
- J. Zhang. Causal reasoning with ancestral graphs. *Journal of Machine Learning Research*, 9(47):1437–1474, 2008.
- Y. Zheng, B. Huang, W. Chen, J. Ramsey, M. Gong, R. Cai, S. Shimizu, P. Spirtes, , and K. Zhang. Causal-learn: Causal discovery in Python. *Journal of Machine Learning Research Inference*, 25(60):1–8, 2024.